Infrared spectroscopy to understand the effect of sodium and sulfur on catalytic performance of supported iron catalysts for the Fischer-Tropsch synthesis of lower olefins

Master Thesis by Jasper B. F. Hooijmans

Supervisors: Jingxiu Xie (JX)
Prof. Dr. Ir. K. P. De Jong
Department of Chemistry
Inorganic Chemistry and Catalysis Group
Utrecht University
June 2015

Abstract

Sodium and sulphur are known to promote the catalytic performance of iron-based catalysts, but their effects are not yet fully understood. In this study, IR spectroscopy was utilized to attempt to shine a light on this effect. Both promoted and unpromoted zirconia-supported iron catalysts were prepared and their catalytic performance compared. As expected, the addition of promoters significantly improved the catalytic activity and selectivity. Zirconia as a support was deemed effective but not superior to the more common α-alumina support. IR spectroscopy results supported by Mössbauer spectra indicated that the promoters do not change the binding energy of CO to the catalyst surface, but instead affect the relative amount of different CO-available binding sites. TPR and Mössbauer spectroscopy also determined that the addition of the promoters improve the rate of reduction.

Table of Contents

Introduction: 4
Methods: 13
Experimental procedures: 14
Results & Discussion: 17
Conclusions 36
Future outlook: 37
Acknowledgements: 38
Bibliography: 39
Supplementary data: 42

Introduction:

The modern-day world is built on the usage of oil. It not only fuels our energy and transportation needs, but is also a source of many crucial base chemicals such as oxygenates and short-chain alkenes. Refineries distill and crack crude oil into the diverse fractions, producing asphalt, waxes, fuels and small-chain base chemicals. Some have straight-forward uses, others continue on a pathway to form more complex end products. Ethylene, propylene and butylenes, together known as lower olefins or C2-C4 olefins, are key base building blocks in the chemical industry, and are among the most produced organic chemicals by volume in the world[1]. Their main uses are polymerization to form some of the most widely used plastics, usage in the production of other important base chemicals or in the synthesis of fine chemicals.

As the world develops, demand for fuel and chemicals continues to increase; however, the amount of oil economically viable to extract from the earth is limited even if the volatility of the oil prices continuously influences the interest in less conventional oil sources such as tar sands, shale oil or arctic drilling sites. The point at which oil production cannot keep up with demand and starts to decrease is expected to follow somewhere in the coming 50 years, even if this horizon keeps shifting as alternative processes are developed or become economically viable. Although the focus on developing alternative energy sources, such as wind, tidal, hydro or solar, is prominent in the mainstream conscience and vital to continue to provide our energy demands, separating our base chemical production from its oil dependency is an equally important but altogether different process that is ongoing. Efforts are made to diversify the feedstock from which they are obtained. Currently, lower olefins are mainly produced through thermal steam cracking of refinery runoffs like naphtha. Steam cracking to obtain lower olefins is one of the most energy-consuming processes in the petrochemical industry and therefore from an environmental and economic standpoint a replacement feedstock or production technique could be invaluable. Foremost among the candidates for the (partial) replacement of crude oil are other fossil fuels such as coal and natural gas; however as the push for sustainability and environmentally friendly processes gains strength the use of biomass as feedstock is increasingly taking center stage. By producing base chemicals from biomass that does not compete with the production of foodstuffs, you obtain a low-cost, carbon-neutral feedstock.

While lower olefins can be obtained from oil through steam cracking and from natural gas by dehydrogenation, alternative feedstocks such as coal and biomass require the breaking down of the carbonaceous material by gasification, or alternatively for biomass, through conversion to alcohol. Gasification produces a mixture of CO and H_2 which is known as synthesis gas or syngas. Syngas is a versatile gas mixture as it can serve as a key intermediate, able to be transformed into many different valuable hydrocarbons through a variety of methods, serving as the building block for the production of a variety of base chemicals. Syngas-reliant processes have a major advantage over petroleum-based production, namely that the produced chemicals are practically free from contaminants such as sulfur, nitrogen or aromatics. These contaminants poison catalysts used further down the chemical production line, cause corrosion of engine parts, make fuel less efficient and cause more pollution.

One of the main processes to produce hydrocarbons from syngas is the Fischer-Tropsch reaction, which was developed in 1925 by two German scientists for whom the process is named. It is a heterogeneous catalytic process, using a solid catalyst to transform synthesis gas into liquid or gaseous hydrocarbons, usually focusing on the fraction most suitable as fuel. The process has been commercially implemented in cases where crude oil was in low supply or alternative fossil fuels were cheaply and abundantly available.

$$(2n + 1)H_2 + nCO \rightarrow C_nH_{2n+2} + nH_2O$$

$$2nH_2 + nCO \rightarrow C_nH_{2n} + nH_2O$$

Equation 1: General reaction equations of the Fischer-Tropsch reaction

The mechanism by which the reaction occurs has been intensively investigated, however it has not been decisively elucidated yet. The general consensus is that the Fischer-Tropsch reaction behaves as a surface-polymerization reaction, resulting in a product distribution instead of a single component. It is generally accepted to be a hydrogenation reaction of CO, with dominant theories placing the cleaving of the C-O bond at differing places in the mechanism[2]. CH_x monomers are formed on the surface of the catalyst which polymerize until chain termination occurs, with H_2O formed as a side product, as shown above in Equation 1.

The Anderson-Schultz-Flory (ASF) distribution shows the expected product distribution by weight by plotting the chain growth probability to show the relative amounts of different products that is produced. The chain growth probability is influenced by a variety of factors such as the process conditions, the type of catalyst used and added promoters.

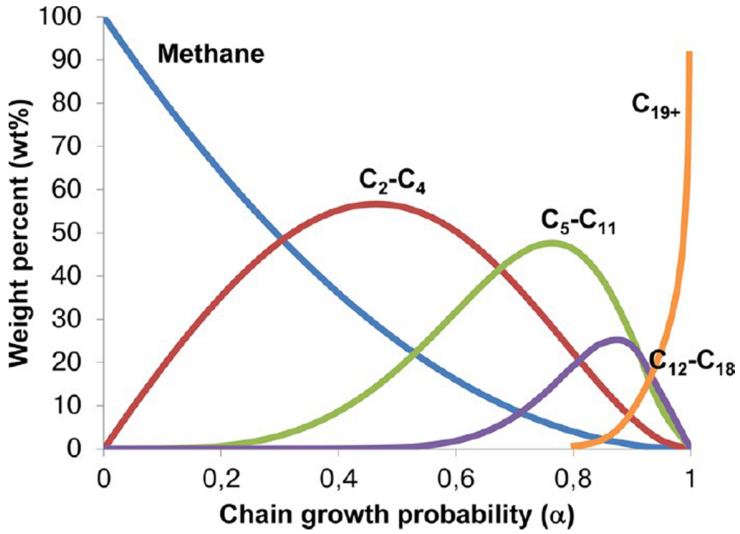

Figure 1: Product distribution based on the Anderson-Schultz-Flory equation[1]

The Fischer-Tropsch reaction can be catalyzed by a variety of metals or alloys, in supported nanoparticulate form or bulk phase. According to the Sabatier principle, a catalyst has to be balanced between opposing characteristics to achieve the optimal activity. For a surface reaction such as Fischer-

Tropsch, a balance between high adsorption rate and strong dissociation activity of CO is required. Group 3-6 metals exhibit strong dissociation activity but have a limited desorption rate, whilst transition metals to the right of the periodic system favour associative adsorption and thus are also not active. Therefore, the main candidates in terms of effectivity are iron, cobalt, ruthenium and nickel. Ruthenium, although an effective catalyst, is usually ruled out outside of a research environment due to its scarce and thus expensive nature. Nickel strongly favours methane formation and therefore is impractical as well. Therefore, generally considered for catalysts are iron and cobalt, both with their own strengths and weaknesses.

Iron is abundantly available and economically attractive for use as a catalyst. It favours the production of olefins and oxygenates due to a lower hydrogenation activity. It is a flexible catalyst, as it can be tuned to produce high weight hydrocarbons or aimed at the production of short-chain olefins, and it is more resistant to catalyst poisons such as sulfur than cobalt. It also has a lower methane selectivity at high temperatures and is therefore more suited for high-temperature operation. Iron is used in a precipitated or fused bulk phase in commercial reactors, whilst research on supported variants is ongoing. A possible advantage of iron is its activity for the water gas shift reaction (WGS) which is shown below. This means that it can be employed for the conversion of CO-rich feedstocks such as from biomass or coal, without the need for an additional gas-ratio adjustment step. Iron is not without its downsides however, as it suffers from low stability; carbon deposition through the Boudouard reaction is a distinct problem that deactivates the catalyst, and it also generally displays a lower activity than cobalt.

$$CO + H_2O \rightleftharpoons H_2 + CO_2$$

Equation 2: The water-gas shift reaction

Cobalt is highly active as a Fischer-Tropsch catalyst and deactivates more slowly than iron-based catalysts. It was initially used in the application of the reaction after its introduction and is nearly always supported on a metal oxide support. It produces mainly paraffins and is generally applied for the production of longer-chain products such as liquid fuels and waxes in low-temperature Fischer Tropsch. A distinct difference between iron and cobalt is the nature of the active phase. Cobalt is active for the Fischer-Tropsch synthesis in the metallic state, whilst for iron the active phase is generally accepted to be iron carbide. This is a simplification however, as there is usually a complex mixture of different phases of iron carbides, oxides and metal present during reaction and research is ongoing to determine the exact nature of the iron active phase[3–6].

$$2\,CO \rightleftharpoons C + CO_2$$

Equation 3: The Boudouard reaction

The catalytic systems used for the Fischer-Tropsch reaction are either supported catalysts or in bulk phase. As stated earlier, cobalt is usually supported on a metal oxide support whilst iron is used in a precipitated or fused bulk phase in commercial reactors, with research on supported variants ongoing. Precipitated iron catalysts can suffer from poor mechanical stability due to formation of carbon filaments formed by the earlier mentioned Boudouard reaction. In theory, a supported catalyst could offer many advantages. It may be better suited to withstand the mechanical degradation and potentially boasts

higher catalytic activity through enhanced dispersion of the active phase. However, they suffer from difficulties in the activation of the catalyst due to metal-support interactions.

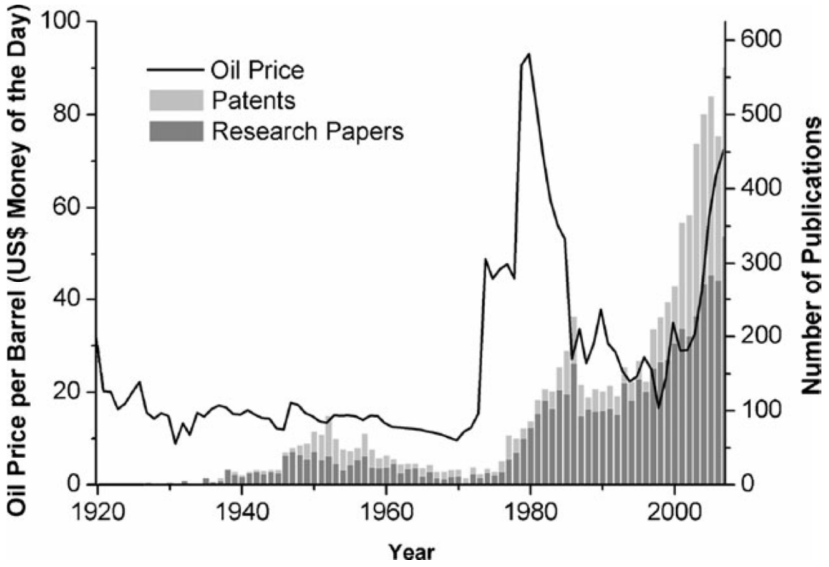

Figure 2: Oil price related to patents and articles published per year[3]

The interest in the Fischer-Tropsch process has waxed and waned in the time since its development, with increasing research efforts coinciding with crises in oil production or availability. The process would be economically viable only if the crude oil price rose significantly, keeping in mind the requirement for infrastructure, which for oil is well-developed and in place in the form of numerous refineries whilst for the Fischer-Tropsch synthesis new plants would have to be built or existing plants converted, greatly increasing the initial cost. For most of the 20th century this was never viable due to the abundance of cheap oil. Exceptions include WWII Germany which lacked oil supplies but had domestic coal reserves, and South Africa under oil sanctions in the 1970s-80s. Global oil crises also caused spikes in research papers and patents on the subject, indicating the renewed interest, as shown in Figure 2. The steadily increasing oil price, instability in oil-producing regions and increasing awareness of the limits of oil production during the last decade or two have once again pushed FTS to the forefront, with academic and industrial interest rapidly increasing to the point of FTS plants being constructed for the conversion of natural gas or coal to liquids.

These revivals however have usually been focused on the production of fuel fractions. A separate development is aiming the reaction towards shorter chains to obtain previously mentioned building block chemicals. The Fischer-Tropsch to olefins (FTO) process is a derivative of the Fischer-Tropsch process, tailored to limit as much as possible its product distribution to lower olefins and could be capable of providing the production of these base chemicals and supporting the growing demand.

The catalysts for this process are almost always iron-based as iron has a higher selectivity towards olefins than cobalt, it produces less methane at the high temperatures required for the process

and as a raw material it is much less expensive, although cobalt is also rarely investigated. Furthermore, FTO is performed at a higher reaction temperature than regular FTS, in order to drive the chain growth probability down towards the smaller chain lengths.

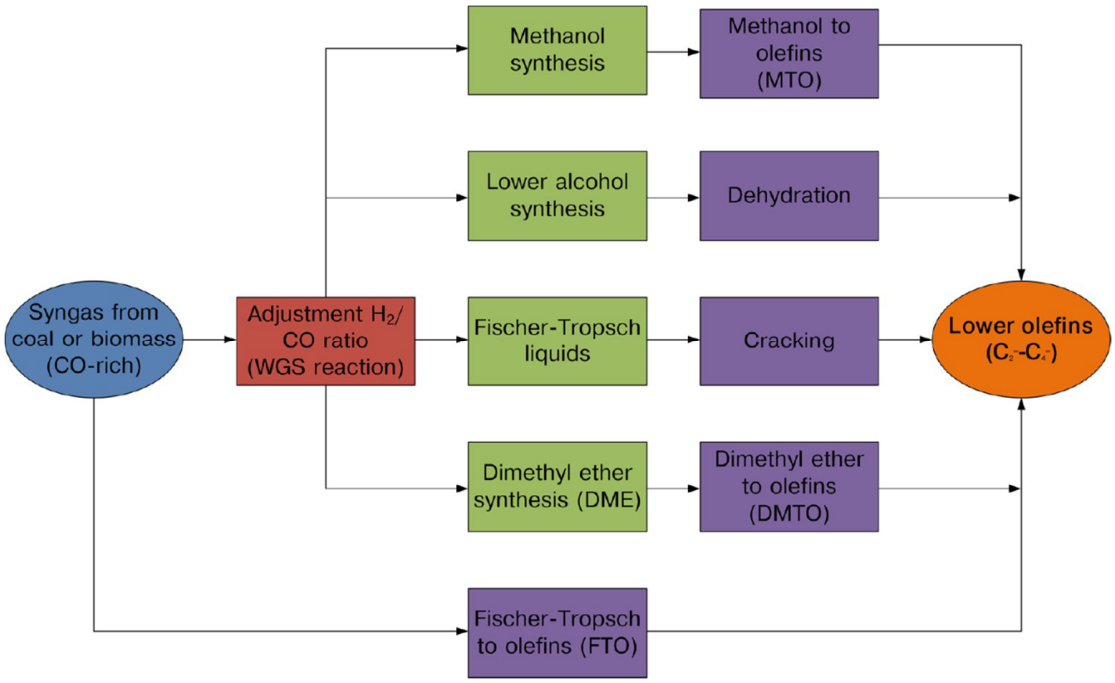

Figure 3: Transformation routes of alternative feedstock-obtained syngas to lower olefins[1].

The FTO process is, in contrast with other methods, a direct process from syngas to lower olefins. As shown in Figure 3, several syngas-employing methods have been developed to produce lower olefins, although they do so through other chemicals. Methanol-to-olefins, or MTO, has been commercialized and with high selectivity produces a mixture of light olefins from methanol which itself is produced directly from methane or from syngas. DMTO (dimethyl ether-to-olefins) is a somewhat similar process to MTO which has the potential to be more efficient as the production of dimethyl ether from syngas is thermodynamically more favourable than methanol, but is still in development. Another possibility is the production of liquid hydrocarbons with the Fischer-Tropsch process followed by traditional cracking to obtain contaminant-free olefins. This makes use of existing infrastructure whilst enabling feedstocks other than oil, but still uses the energy-intensive cracking procedure.

The benefits of a direct process are clear; no transition in reaction conditions, less complexity due to the need for only one reactor and one catalyst all add up to economical and practical benefits to having a single, direct process from feedstock to desired product. Despite this, FTO has not yet been commercially implemented. This is due to a critical issue in the reaction, namely that with a low chain growth probability that results in the highest amount of C2-C4 olefins produced a very significant fraction of methane is also produced, as can be seen in Figure 1, which is an unwanted side-product. To make the reaction viable the methane fraction must be reduced.

Catalysts can often be improved by the addition of materials or elements that promote their workings. Elements that facilitate the reduction, structural promoters or improve the selectivity or activity are key additions to Fischer-Tropsch catalysts[7]. The promoters usually only confer their improvements when added in low concentrations and act as poisons in increased amounts. Unpromoted or unmodified iron catalysts suffer from poor selectivity, low activity and sintering. Precipitated iron catalysts are often modified with a structural modifier such as Si, Al or Mg for added strength and stability[8], whilst supported iron catalysts rely on their supports for this. Alkali metals are known to increase the chain growth probability and lower methane selectivity and are a staple for iron-based catalysts. Several other elements have been suggested as having a positive effect on the catalysts. Metals such as Cu or noble metals can be added to enhance the reduction step. Alkaline earth metals inhibit the reduction, but facilitate the carburization of iron and inhibit the hydrogenation of carbon[9]. A number of different transition metals such as Mn, Zr, Cr or Mo among others have been investigated with varying results, reporting increased hydrogenation and WGS activity, and iron dispersion[10]. Sulfur is, although long known as a catalyst poison, also investigated as a promoter when added in low concentrations[11,12].

Previously, Torres Galvis *et al.*[13] reported a supported iron catalyst promoted with sodium and sulfur for Fischer-Tropsch reactions at high temperature. This catalyst displayed high activity, stability and selectivity for lower olefins. In a follow-up paper, they discussed the effects of these promoters on the catalytic performance[14]. Sodium increased the chain growth probability, thereby decreasing methane selectivity. Sulfur enhanced the catalytic activity, decreased methane selectivity and increased lower olefins selectivity, which they speculate was caused by sulfur possibly reducing the hydrogen coverage of the catalyst, restricting the termination of chain growth through hydrogenation and thus increasing the β-hydride elimination termination probability. A key observation was that the promoters led to a deviation from the predictions of the ASF model, as a less methane was produced than the distribution predicts. In the previously mentioned follow-up paper, a 5wt% iron on α-alumina promoted with both sodium and sulfur produced 19% methane and 51% C2-C4 olefins whilst a catalyst without these promoters produced 27% methane and 35% C2-C4 olefins in the Fischer-Tropsch reaction (20 bar, 340°C, $H_2/CO=1$)[14]. This ability to obtain high olefin fractions whilst keeping methane production down greatly enhances the industrial potential of the FTO process.

However, these promoter effects still requires more investigation to fully determine their origin and cause. Understanding the origin of these promoter effects can be very valuable as the catalyst can then be further improved by building upon this knowledge instead of empirical proof and ideally be optimized for industrial use. One technique that can potentially shine a light on the effect of the promoters is infrared spectroscopy, which is commonly used to study the interaction of molecules with catalysts and their active phases[15]. If the promoters affect the adsorption and interaction of reactants with the active phase, IR could illuminate this.

IR spectroscopy can be very effective when studying the surface of a catalyst, especially when employing probe molecules such as CO. When CO associatively adsorbs to a metal surface, the metal-carbon bond adds electrons to the anti-bonding orbital of the molecule, lowering the binding energy of the carbon-oxygen bond and thus lowering the wavenumber at which the molecule absorbs IR radiation. Gaseous CO absorbs at 2175 and 2114 cm^{-1}, but the wavenumber of adsorbed CO is typically between 2100 and 1800 cm^{-1} depending on whether the molecule is linearly, bridged or multiply bonded to the surface, as the CO bond energy is lowered by backdonation when bonded to a surface[16]. Using this, information can be obtained on how strongly CO is bonded to the surface, what kind of adsorption sites are available and, through comparison between unmodified and promoted catalysts, whether the promoters in any way influence the way molecules are adsorbed.

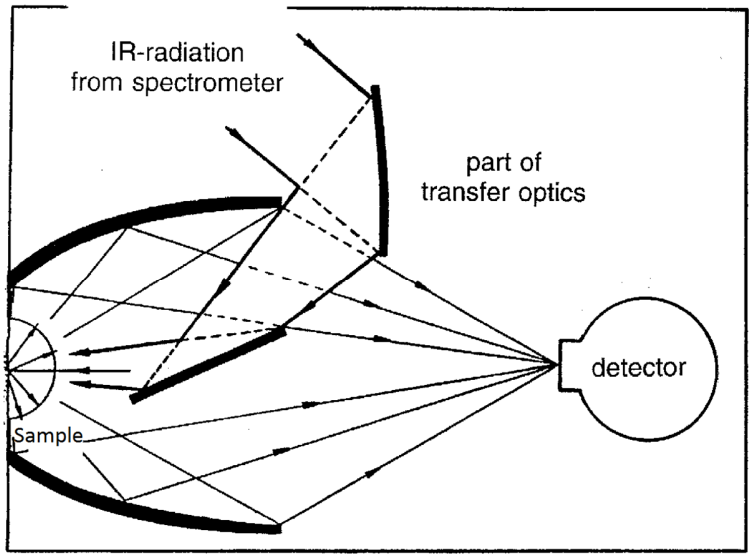

Figure 4: General schematic of a DRIFTS setup[33]

Diffuse Reflectance Infrared Fourier Transform Spectroscopy, or DRIFTS, is a spectroscopic technique that is often used as an alternative to traditional transmission IR spectroscopy when a sample scatters too strongly or otherwise prevents light transmission. Instead of illuminating through the sample as with transmission IR, the IR beam is directed onto the sample and as much of the diffusely reflected radiation as possible is redirected towards the detector as illustrated in Figure 4. This is valuable when studying samples such as catalysts using a metal oxide as a support as these materials often have a strong light scattering ability. A downside of DRIFTS is that it is impossible to capture all reflected light; this means that the signal is relatively lower than other IR spectroscopic techniques. DRIFTS is commonly used in concert with a probe molecule such as CO, allowing for the study of its interaction with the sample surface. Samples are measured in powder form, meaning pretreatment is much more facile and allows for better diffusion than the pellet method commonly used in transmission IR. This means that the technique is well-suited to studying oxidic supported Fischer-Tropsch catalysts, as DRIFTS allows for the study of the surface interactions even on highly reflective samples. However, important to remember is that in order for the Fischer-Tropsch reaction to occur, CO has to dissociate. Thus,

measurements under full reaction conditions are likely to provide much less signal than CO adsorption at low temperature.

DRIFTS has been widely applied to study the effect of promoters on iron and cobalt Fischer-Tropsch catalysts. Curtis *et al.*[17] and Morales *et al.* [18] employed DRIFTS to study sulfur and manganese promoters on cobalt catalysts, respectively. Curtis showed that sulfur appeared to reduce the CO coverage on cobalt, whilst Morales reported that the addition of manganese relatively increased the amount of linearly bonded CO on cobalt, indicating an electron-withdrawing effect on the metallic cobalt. Jiang *et al.* [19] studied precipitated iron catalysts with or without manganese. They found that CO probes only gave rise to very weak bands on reduced iron samples, indicating their dissociation. Samples containing manganese did show well-resolved bands, possibly due to a increased iron particle size in reduced samples. Kazansky *et al.*[20] used DRIFTS to study the effect of alkali promoters on alumina supported iron and cobalt catalysts, and determined, through a change in intensity of CO peaks bonded with Fe or Co ions compared to metal-bound CO between unpromoted and promoted samples, that the additives stabilized the metallic forms.

Thus, DRIFTS may be well suited to study the reported promoter effect of sodium and sulfur. This then is the goal of this study; to investigate the effect of the sodium and sulfur promoters on a supported iron catalyst for the FTO process, employing IR spectroscopy to study the possible differences between unpromoted, singly promoted and doubly promoted catalysts and correlate this to their activity and selectivity.

The various aspects of the desired catalyst were adapted to the goals of this research; it was not necessary to obtain the catalyst with the best catalytic performance. Instead, attention was focused on obtaining a strong IR signal and if the synthesized catalysts exhibited the effects of the promoters in order to be able to study them. Optimizing the available adsorption sites is key. To accomplish this, the weight percentage of iron added must be balanced in such a way that the IR signal is optimal. Too low an iron loading might result in insufficient available adsorption sites for CO to study the interaction, whilst too high a loading could result in the formation of large iron particles, also lowering the available surface for CO probes to adsorb.

Using ammonium iron(III) citrate as precursor for the iron particles in the catalyst preparation is reported to result in a uniform dispersion of very small iron oxide particles due to the chelating anion, in contrast to the extensive clustering observed when using iron nitrate[21]. An added merit of the iron precursor may be that after calcination some carbonaceous material may be left from the decomposition of the citrate and this can help prevent formation of large iron oxide particles[22]. These carbon deposits could also increase the rate of carburization, as whenever metallic iron is formed during the reduction, this can immediately react with the carbon present[23].

The choice of support is significant as well, as it could potentially inhibit the promoter effect or interfere with obtaining a sufficient IR signal. Common supports are usually metal oxides, such as silica, alumina or titania. These are stable, hard to reduce materials and usually mechanically strong, although this depends on the actual structure of the support. However, they often exhibit strong metal-support interactions, hindering the formation of active phase by stabilizing the iron oxide phase or forming

difficult to reduce alloys like iron(II) silicate or aluminate[8], requiring a low surface area to limit these effects, such as α-alumina. Carbon-based supports are ruled out despite their high activity and selectivity in earlier studies on the basis that they strongly absorb IR radiation. Weakly interacting supports are preferred, offering enough interaction to anchor the catalytically active nanoparticles and limit sintering whilst not inhibiting the formation of the active phase or their activity. Aggregation of the active phase severely limits catalytic activity and could lead to increased methane selectivity.

Zirconia as a support material could prove promising[22,24,25], as it is reported to exhibit weaker metal-support interactions than other more commonly used oxidic supports, not forming bulk iron(II) zirconate during reduction, as opposed to the prevalent formation of iron(II) silicate or aluminate from their respective supports. It also has limited interaction with alkali metal oxides, ensuring this promoter should be present mostly on the iron particles. Compared to α-alumina, zirconia supports also have a higher surface area and thus should provide a higher signal in DRIFTS. As the above-mentioned metal-support interaction should be weaker, this higher surface area should not inhibit the catalyst's effectiveness as strongly as seen when comparing α-alumina and the higher surface area γ-alumina. These properties indicate zirconia could potentially be a suitable and effective support for a promoted iron-based FTO catalyst, and this will be investigated by comparing both promoted and unpromoted α-alumina- and zirconia-supported catalysts, alongside its use in the study of the promoter effects.

Methods:

Mössbauer spectroscopy[26]:

Mössbauer spectroscopy is a powerful but specialized technique that can offer information about the magnetic properties, chemical surroundings and oxidation state of the material of interest. It is a specialized technique because it can only be used for a limited number of elements such as Fe, Sn or Sb among a few others. This limitation stems from the effect it is based on and named after, the Mössbauer effect, also known as nuclear gamma radiation resonance.

Free atoms, or atoms in a gas experience recoil when emitting a photon. However, when an atom is bonded in a crystal lattice, its ability to recoil is severely reduced as the whole lattice receives the recoil energy and its effect can become negligible, meaning that recoil-less adsorption or emission can occur. This means that the resonance effect can be observed.

Through radioactive decay, gamma-radiation of a very defined energy is emitted by a source. As the nuclear transition energies of emission and adsorption are the same, in theory this photon fits a nuclear energy transition of the same element in the sample of interest. However, the chemical environment of an atom influences the nuclear energy levels, shifting or splitting them by hyperfine interactions and thus changes the exact energy of the transition. This is what makes this effect interesting for the study of materials, as the minute changes in energy of the transition gives information about the chemical and magnetic state of the sample.

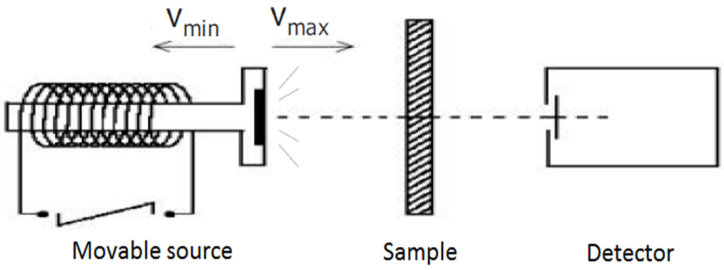

Figure 5: General schematic of a Mössbauer spectrometer[27] (chapter 4.6)

In order to study these minute changes, you need to be able to vary the energy of your source, which has a very sharp output. This is done by the use of the Doppler effect. Moving the source towards or away from the sample red- or blueshifts the energy of the emission, enabling the covering of these changes in energy. Typically, for iron, the velocity of the source required to study all shifts covers a range of -10 to 10 mm/s. This is the basis of Mössbauer spectroscopy, as shown in the schematic above.

Experimental procedures:

Synthesis:

Incipient wetness impregnation (IWI) was utilized to prepare the supported iron catalysts. The supports employed, of which details can be found in Table 1, were ground and sieved to a 212-425 µm size beforehand. Unpromoted, singly promoted and doubly promoted catalysts were prepared in identical fashion. Ammonium ferric citrate, ferrous sulfate and sodium citrate tribasic were used as the precursors for the iron oxide, the sulfur promoter and the sodium promoter respectively. As mentioned previously, iron citrate as a precursor is preferable over iron nitrate as it results in improved dispersion of the iron. The desired loading of the promoters was 0,22wt% of Na and 0,03wt% of S for a catalyst containing 5wt% Fe, or double these amounts for 10wt% Fe loaded samples. In a typical impregnation to obtain a 5wt% iron, doubly promoted catalyst, a precursor solution was prepared by simultaneously dissolving 0,696g of ammonium ferric citrate (Fluka analytical, p.a., 14,5-16% Fe), 0,005g of ferrous sulfate heptahydrate (Merck, p.a.) and 0,020g of sodium citrate tribasic (Sigma-Aldrich, ACS reagent, ≥99,0%) in 0,9mL of demineralized water. This precursor solution was then added dropwise to 2,0g of support in ambient pressure until the pores were filled, after which it was dried for 1h at 120°C in static air. These steps were repeated until all of the solution had been added to the support. Afterwards, the sample was dried for 2h at 120°C in static air before calcining at 500°C for 2h in flowing air (10°C/min heating ramp). It was assumed that all prepared catalysts achieved their theoretical loading unless stated otherwise. All prepared samples were clearly rust-coloured after calcination, suggesting the presence of iron oxide. Sample labeling was done according to the following convention: "support-iron loading/promoters", meaning that Zr1-Fe5/Na/S is a catalyst containing 5wt% iron with both Na and S promoters on the SZ39140 zirconia support.

Table 1: Properties of the employed supports

Manufacturer		Support	Crystal phase	Impurities	Surface area (m^2/g)	Pore volume (mL/g)
BASF	Al-4196E	α-Alumina (αAl)	α	-	8	0,5
Norpro	SZ39140	Zirconia (Zr1)	Mixed monoclinic/tetragonal	Contains 40% anatase(TiO_2)	80	0,46
Norpro	SZ31163	Zirconia (Zr2)	Monoclinic	<0.2% SiO2	55	0,3
Norpro	SZ61156	Zirconia (Zr3)	Tetragonal	Contains 10% La_2O_3	120	0,3
Norpro	SZ31164	Zirconia (Zr4)	Monoclinic	<0.2% SiO_2	85	0,29

Characterization:

Fresh catalysts were characterized using X-ray diffraction and transmission electron microscopy, to investigate whether the impregnation was successful and did not influence the structure of the support and to determine the particle size distribution. X-ray diffractograms were recorded on a Bruker D2 Phaser equipped with a Co Kα source (λ = 0.1789nm), measuring from 20° to 80° 2θ with 0,08° increments. TEM images were taken on a Philips Tecnai-12 (120 kV), with additional high resolution and STEM-HAADF imaging and TEM-EDX measurements performed on a Philips Tecnai-20 (200 kV). For TEM imaging, the contrast between the iron oxide particles and the support was expected to be poor because the zirconium in the support material is heavier than iron. Therefore, where necessary EDX measurements were employed to distinguish between the two. Both fresh and spent catalysts were imaged with TEM to compare and investigate the effect of the reaction conditions on the catalyst, such as iron particle formation and/or growth and carbon deposition.

Temperature Programmed Reduction was performed to investigate the effect of promoters on the reduction of the catalyst. In a Micromeritics Autochem II 2920, 50 mg samples were heated to 500°C at 5°C/min under a 50 mL/min flow of 5 vol.% H_2/Ar. The hold time at final temperature was differentiated because of unknown extent of reduction.

The DRIFTS measurements followed the same catalyst activation procedure as the FTO catalytic testing to ensure that the resulting spectra and catalyst testing results can be related. Measurements were performed on a Thermo Nicolet Nexus 470 FT-IR spectrometer equipped with a Smart Collector DRIFTS accessory with ZnSe windows. The sample was finely ground to maximize the amount of reflective surface. After loading the cell with approximately 30mg of sample, it was brought up to 350°C at 5°C/min under 40 mL/min He flow. Next followed reduction of the sample for 2 hours at this temperature under a mixture of H_2 and He or of CO and He(33% H_2 or CO v/v, 60 mL/min), with a 15 min desorption step under 40 mL/min He afterwards. Next, it was cooled down to room temperature by switching off the heating element, and after stabilizing a background spectrum was recorded (resolution 4 cm^{-1}, 128 scans). The measurement was started at the same time as CO probe adsorption was begun at room temperature for 30 minutes (40 mL/min CO), after which the desorption was monitored by switching to 40 mL/min He. Spectra were recorded continuously to monitor the change over time of peaks during adsorption and desorption. Spectra were recorded from 4000 to 400 cm^{-1} with a resolution of 4 cm^{-1}, accumulating 128 scans per spectrum.

To corroborate the DRIFTS data, Mössbauer spectra were recorded to determine the phases present during the various steps of activation and CO adsorption by replicating the DRIFTS procedure. Transmission ^{57}Fe Mössbauer absorption spectra were collected at room temperature with a conventional constant-acceleration spectrometer using a ^{57}Co(Rh) source. Velocity calibration was carried out using an α-Fe foil. The Mössbauer spectra were fitted using the Mosswinn 4.0 program.

Catalytic testing:

Testing the catalyst performance was done by running the Fischer-Tropsch synthesis at 1 bar and 350°C in a fixed bed. 20 mg of catalyst was mixed homogeneously with 200 mg of SiC as bed dilution, both with a particle size of 212-425 µm, and placed in a plug-flow reactor. Prior to reaction, the sample was brought to 350°C at 5°C/min under a flow of 40 mL/min He and reduced at that temperature for 2 hours after switching the gas flow to a mixture of H_2 and He (33% H_2 v/v, 60 mL/min). After reduction, the gas flow was changed to a 1:1 syngas mixture (6 mL/min) for the reaction, which was carried out for 20 hours. The products were analyzed by online gas chromatography.

Additionally, 20 bar catalytic testing was done to observe the presence of the promoter effects on more industrially relevant conditions. The 20 bar Fischer-Tropsch reaction was performed in a high throughput fixed-bed reactor under a 8 mL/min $CO/H_2/He$: 45/45/10 composition gas flow at 340°C. The sample was prepared by diluting 40 mg of catalyst with 200 mg of SiC. No reduction step was performed before reaction. Product selectivity up to C_9 was determined by online gas chromatography.

Results & Discussion:

Zirconia as a suitable support:

As was put forward earlier, zirconia was expected to exhibit favourable properties as a support material for a Fischer-Tropsch catalyst in general, forming no bulk iron-support phases such as iron silicate or aluminate and not interacting with alkali metal oxides, and IR studies specifically, possessing a higher surface area than α-alumina. In order to investigate its suitability, four zirconia supports were obtained from a supplier which varied in their properties, which are summarized in Table 1, to compare which would be most suitable as a catalyst.

Initial zirconia testing:

Zr1 was used as a support in a pilot where an unpromoted and a doubly promoted catalyst with a 5wt% iron loading were prepared in order to observe whether the promoter effect was not inhibited by the zirconia support, if this iron loading was sufficient to provide sufficient intensity returns in IR investigations and to investigate the structure of the catalysts based on zirconia.

Shown below in Figure 6 are XRD diffractograms of Zr1-supported catalysts after calcination and a blank support for comparison. No additional peaks can be discerned for the prepared catalysts when compared to the blank support. They show no clear iron oxide (hematite) peaks, although the samples are clearly rust-brown coloured. This indicates that the iron oxide present is either amorphous in nature or smaller than the detection limit.

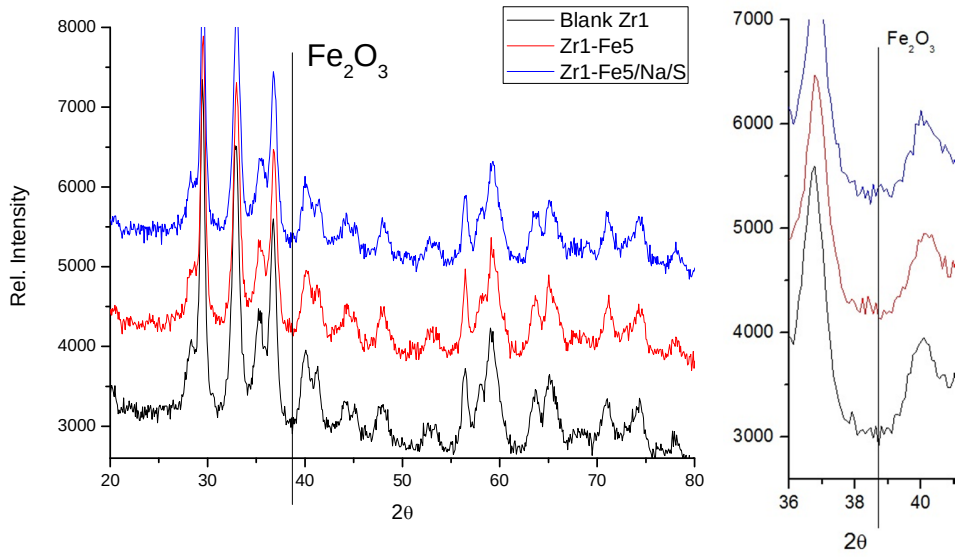

Figure 6: XRD diffractograms of Zr1-supported catalysts with insert showing expected location of highest-intensity hematite peak

Van den Berg *et al.*[22] reported that when ammonium iron citrate is used as the precursor of the iron oxide phase, it may form an amorphous layer on the support instead of discrete particles and thus it may be impossible to determine the iron particle size for zirconia supported samples. To determine whether this is the case, the samples were investigated with TEM.

In the TEM images shown in Figure 7, highly crystalline zirconia crystallites appear to have a 10-20 nm size. No smaller particles or roughness of the particles was observed in the catalysts when compared to the blank support. EDX measurements (spectrum displayed in Figure S1) confirmed that iron was present, however, but were unable to pinpoint its location.

It is possible that the iron oxide phase has entered a solid solution phase with the support material, as monoclinic zirconia is able to accept up to 15mole% of iron oxide without change in structure[28]. This explains the inability to detect iron oxide with XRD or separate particles in TEM. However, this could possibly affect the reduction rate as the zirconia anchors the iron oxide.

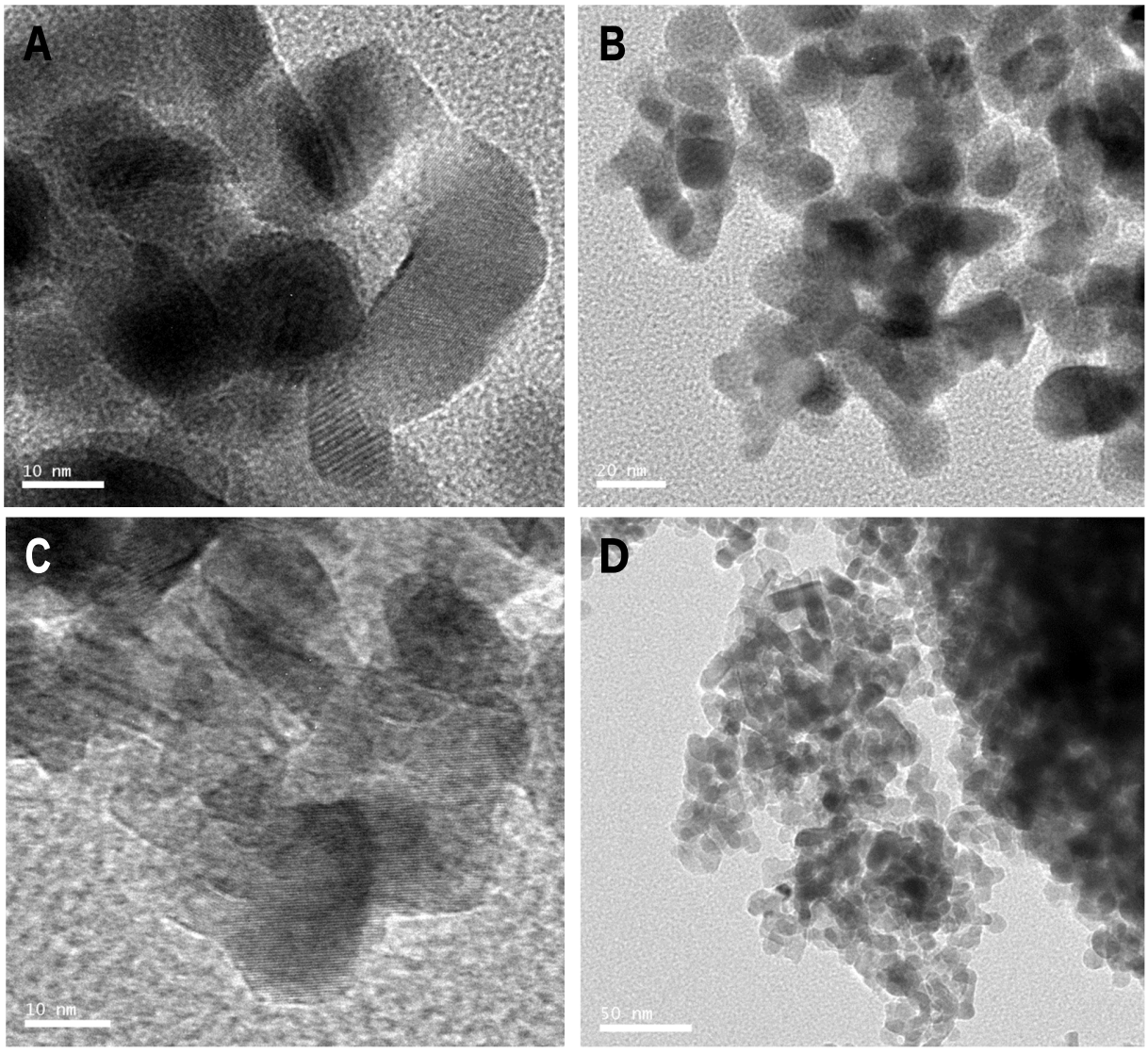

Figure 7: TEM images of Zr1 supported samples showing no significant differences between prepared catalysts (A, B) and untreated support particles (C, D)

Pilot DRIFTS measurements were performed on the Zr1 supported samples to investigate the validity of the support and the iron loading for further IR testing. The resulting spectra, seen below in Figure 8, showed a singular peak at 2007/2009 cm^{-1} respectively, corresponding to CO linearly bound to a metallic surface[16]. Another region of interest is 1700-1200 cm^{-1}, where mono- and bidentate carbonates bound to or trapped within the oxidic support appear[29]. These results provided the confirmation that zirconia was a suitable support for IR investigations, and that 5wt% iron loading was sufficient to provide a workable signal.

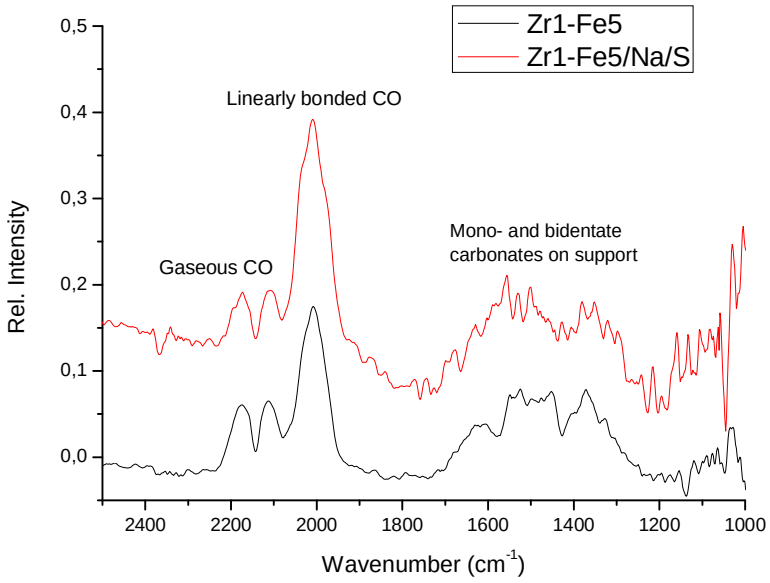

Figure 8: DRIFTS spectra of Zr1 supported catalysts taken 10 min after the start of CO desorption, with peaks and areas of interest labeled

Based on the positive outcomes of the structural pilots, singly promoted catalysts Zr1-Fe5/Na and Zr1-Fe5/S were prepared and the four Zr1-supported samples were tested for their catalytic performance in the 1 bar Fischer-Tropsch reaction. The activity and selectivity over time of these runs are shown below in Figure 9.

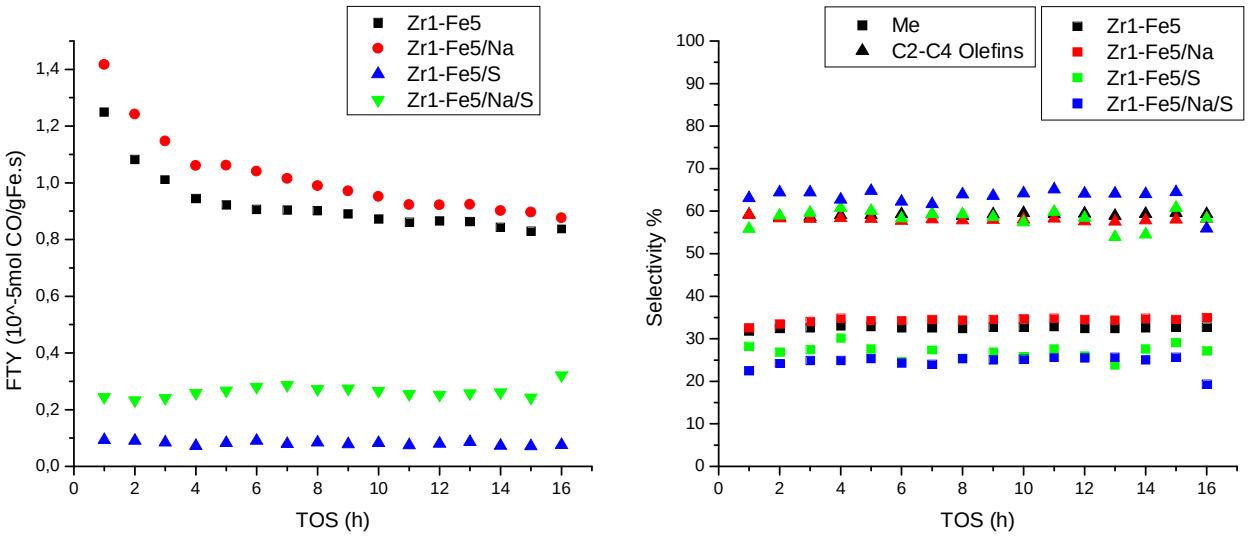

Figure 9: Comparisons of activity and selectivity of Zr1 supported catalysts for the 1 bar Fischer-Tropsch reaction

As can be seen, the unpromoted and the sodium promoted catalysts follow an exponential decay before stabilizing into a slowly deactivating activity trend, whilst both samples containing sulfur display uniformly stable activity. All samples do not deviate in selectivity over time. When compared to the promoted catalysts, the unpromoted sample shows remarkably high activity. The addition of Na slightly improves this activity, whilst the addition of sulfur significantly reduces activity. This could mean that the sulfur loading is too high, as it is considered a poison in higher amounts, or that it does not display its expected promoter effect, only inhibiting. S promoted catalysts do show a marginally improved selectivity, lowering methane selectivity by 5 to 10%, again with the unpromoted sample showing remarkable selectivity. Surprisingly, all catalysts, including the unpromoted catalyst, show a deviation in methane selectivity from what is expected, as shown below in an ASF plot. The sulphur promoted samples' ASF datapoints are erratic due to low activity, which leads to possible errors in integration. The alpha values obtained are near the maximum for C2-C4 selectivity, however the discrepancies from what was expected from the addition of promoters begged further investigation.

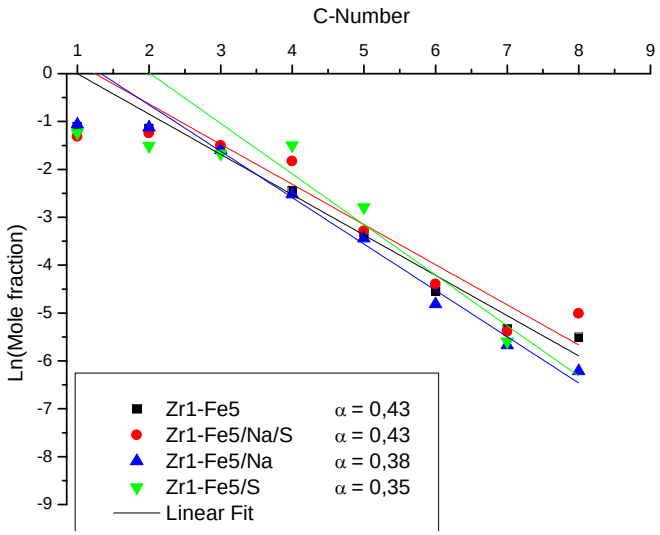

Figure 10: ASF plot of Zr1 supported catalysts with linear fitted trends and α-values

To further investigate the reproducibility of these results, a rerun of unpromoted and a doubly promoted catalyst were synthesized from scratch. These samples were labeled r-Zr1-Fe5 and r-Zr1-Fe5/Na/S respectively. XRD measurements showed that there was no difference in structure between the initial and remade samples, making it likely that the structure of the catalyst before reduction is not responsible for the disparity in activity. However, the catalyst performance differed significantly, as can be seen in Figure 11.

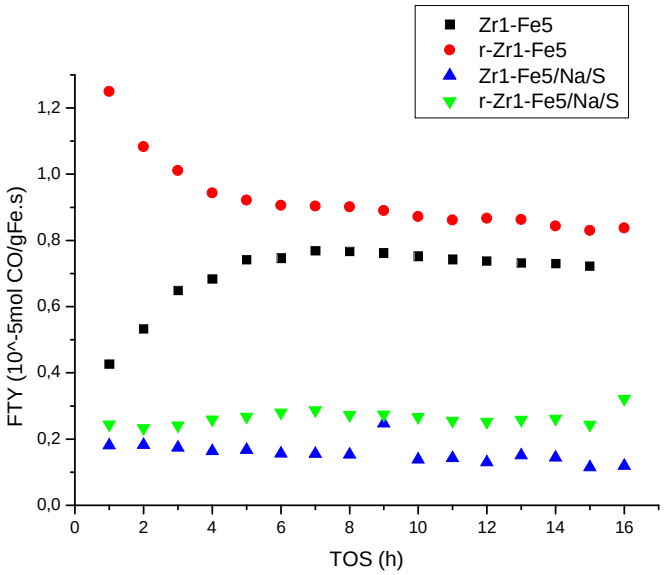

Figure 11: Activity comparison between original and remade Zr1 supported samples in the Fischer-Tropsch reaction

The activity trend of the unpromoted catalysts shows a significant difference. One shows high initial activity, stabilizing after 5 hours on stream to a stable, slowly deactivating state, whilst the other instead shows a 6 hour slow activation period before settling into approximately the same stable deactivation trend. This means that although the resulting activity on stream is roughly equal, the activation stage is very different.

It is hypothesized that the support was contaminated, resulting in irreproducible results. Because of the proposed contamination and reproducibility issues, the Zr1 support was dropped from further investigation.

Zirconia support evaluation:

Due to the aforementioned issues surrounding the Zr1 support three more zirconia supports, denoted Zr2 to Zr4, were employed for a comparison, differing in the areas thought to be likely to influence the active phase or ease of use; different crystal phases could have different strength of metal-support interactions, influencing the activation of iron. Likewise, the surface area of a support can influence the activity of a catalyst, depending on the strength of interaction between the active phase and support. High interaction means that a low surface area is preferred, minimizing its effect on activity, whilst if the interaction is low, a high surface area maximizes the dispersion and therefore activity. Literature values of α-alumina supported catalysts from Torres Galvis *et al.*[14] were used to compare the zirconia supports to a more widely used support.

The XRD diffractograms of the prepared supports can be found in the supporting information. All zirconia-supported catalysts showed no discernable iron oxide peaks, whilst α-alumina-supported samples did show clear hematite peaks.

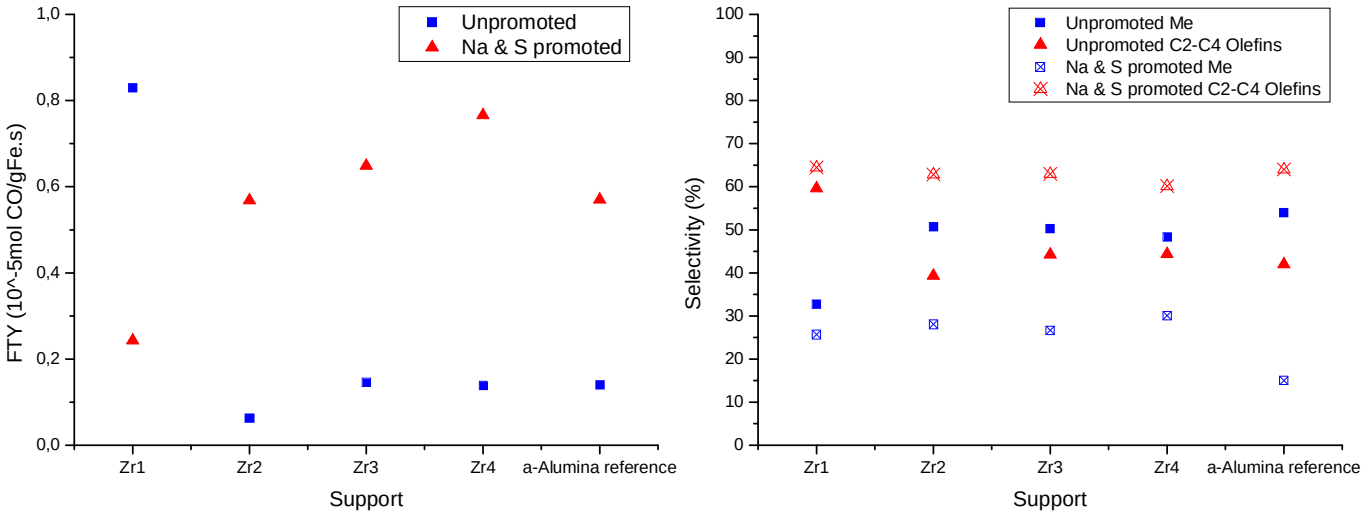

Figure 12: Comparison of activity and selectivity between utilized supports for the 1 bar Fischer-Tropsch reaction after 15h on stream. α-Alumina supported catalyst data taken from Torres Galvis *et al.*[14] for comparison.

The results of 1 bar Fischer-Tropsch testing are summarized in Figure 12 and Table 2. As can be seen, the Zr1 based catalysts show significantly different results than samples prepared on other supports. Furthermore, all other supports show an improved activity and selectivity towards C2-C4 olefins, with methane selectivity dropping across the board. None of the zirconia's can match the selectivity improvement of the reference α-alumina catalysts, although the activity increase is on par or better. This shows that although not the optimal support for catalytic performance, the promoter effect is present and significant, comparable to literature results.

Table 2: Activity and selectivity of both unpromoted and doubly promoted zirconia-based catalysts for the 1 bar Fischer-Tropsch reaction after 15h on stream

Sample	FTY (10^{-5} mol_{CO}/g_{Fe}·s)	Selectivity %			
		Me	C2-C4 Olefin	C2-C4 Paraffin	C5+
r-Zr1-Fe5	0,83	33	60	3	4
r-Zr1-Fe5/Na/S	0,24	26	64	2	8
Zr2-Fe5	0,06	51	39	1	9
Zr2-Fe5/Na/S	0,57	28	63	2	7
Zr3-Fe5	0,15	50	44	2	4
Zr3-Fe5/Na/S	0,65	27	63	2	9
Zr4-Fe5	0,14	48	44	1	6
Zr4-Fe5/Na/S	0,77	30	60	2	8

The irregularities in the Zr1 samples' catalytic performance prompted an investigation into the reproducibility of the FT testing setup results. 5 separately prepared samples of Zr4-Fe5/Na/S were tested on the 1 bar FT setup. Shown in Table 3 are the results of this reproducibility testing. Over 5 separate runs, the standard deviation in selectivity was around 4% from average for methane and 1% for C2-C4 olefins whilst the deviation in activity was around 3% from the average; this shows that the irregularities are unlikely to have been caused by the testing setup and the results obtained from the 1 bar FT setup are reproducible.

Table 3: Results from reproducibility testing of 1 bar FT setup; Samples were prepared and tested individually

Sample	**Zr4-Fe5/Na/S**	Run 1	Run 2	Run 3	Run 4	Run 5	**Average**	**St. Dev.**
Selectivity %	Me	30,1	29,6	30,0	27,5	29,6	**29,4**	**1,1**
	C2-C4 Olefins	60,1	60,9	60,8	59,4	61,1	**60,5**	**0,7**
FTY (10^{-5} mol_{CO}/g_{Fe}·s)		0,766	0,710	0,708	0,750	0,738	**0,735**	**0,025**

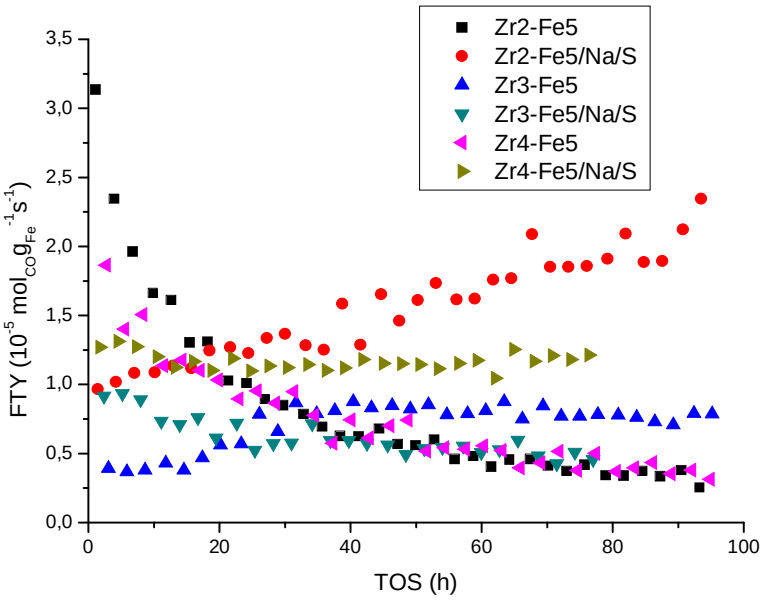

Figure 13: Activity over time of zirconia supported catalysts for the FTO reaction (20 bar, 340°C, H_2/CO=1)

A selection of samples was also tested under more industrially relevant conditions at 20 bar. Above in Figure 13 the activity over time is shown. Selectivity and FTY after 40 hours on stream are summarized in Table 4 as most samples have stabilized at this time, which can be seen in Figure 13. The selectivity of samples that exhibit low (<5%) CO conversion varied over a range of 10-15%, likely due to errors in detection or integration of the GC results. For these samples the selectivity is averaged over several datapoints to eliminate this inaccuracy.

It appears that for the Zr2- and Zr4-supported catalysts the unpromoted catalysts are initially more active but follow an exponential decay in activity, whilst the promoted catalysts are more stable, eventually overtaking the unpromoted samples in activity. The Zr3-supported catalysts, a tetragonal zirconia with 10% La_2O_3 for crystal structure stability, are anomalous in that nature as the unpromoted sample starts of at low activity, but undergoes a (secondary) activation after 10-15 hours on stream, reaching approximately double its initial activity after 30 hours on stream and stabilizing at that level.

Table 4: Overview of catalytic performance of catalysts for the FTO reaction (20 bar, 340°C, TOS=40h, H_2/CO=1). CO_2 is 35-40% of total CO converted; CO conversion is 3-12%.

	FTY ($10^{-5}$$mol_{CO}$/$g_{Fe}$·s)	Selectivity % of total hydrocarbon product		
Sample		Me	C2-C4 Olefin	C2-C4 Paraffin
Zr2-Fe5	0,66	35	30	17
Zr2-Fe5/Na/S	1,44	26	37	16
Zr3-Fe5	0,84	33	29	17
Zr3-Fe5/Na/S	0,58	27	36	20
Zr4-Fe5	0,68	30	33	12
Zr4-Fe5/Na/S	1,14	24	35	18

ASF plots in Figure 14 show that for all three promoted samples, the methane selectivity deviates from the expected value. Due to the small amount of data points only general trends can be considered, α-values are possibly not accurate. It does however show that all samples have a higher chain growth probability than optimal for C2-C4 olefin selectivity. Overall the addition of Na & S promoters results in an average 5-10% decrease in methane selectivity and a similar increase in C2-C4 olefin selectivity. No definitive conclusion can be drawn regarding activity, due to the differing activation/deactivation trends. In the case of Zr2, The promoted sample shows a linearly continuing increase in activity throughout the reaction, whilst the unpromoted sample shows an exponential decline. For the samples supported on Zr3 the promoted sample initially is more active, until the unpromoted sample undergoes a (secondary) activation and becomes more active than the promoted sample. In the case of Zr4, the promoted sample is more stable and thus after 20h on stream more active.

Thus, the promoter effect is still present on zirconia-supported catalysts under more industrially relevant conditions, improving the selectivity of lower olefins whilst lowering the methane selectivity and generally showing increased catalytic activity. The stability of the promoted sample in high pressure testing, solid activity and selectivity increase in low pressure testing and lack of contaminants contributed to the decision to focus on the Zr4 support to continue investigating the promoter effect.

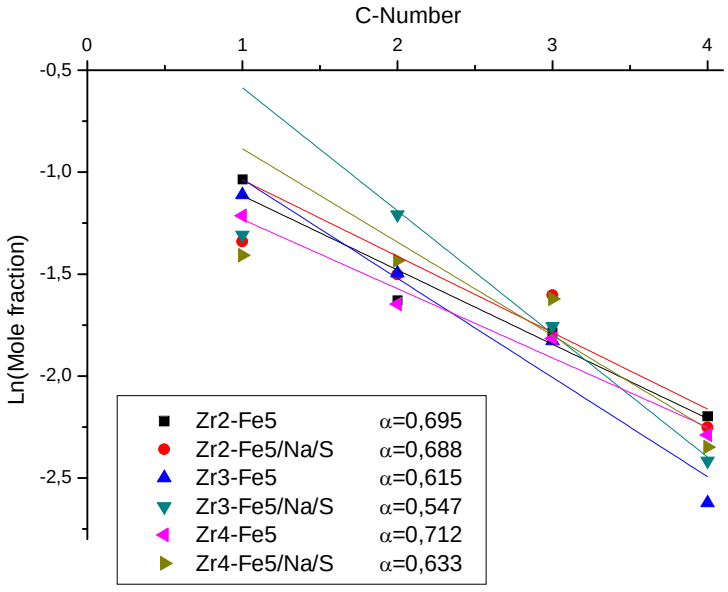

Figure 14: ASF plots of 20 bar FT reaction tested samples, showing linear fitted trends and α values. Methane selectivity deviates from the expected value in all three promoted samples. Selectivity taken after 40h on stream.

Zr4 structural & catalytic testing:

Based on the Zr4 support, singly promoted catalysts and higher iron loading catalysts were prepared to serve as comparisons alongside the unpromoted and doubly promoted 5wt% iron samples in order to further investigate the support validity, stability and the individual effect of the promoters.

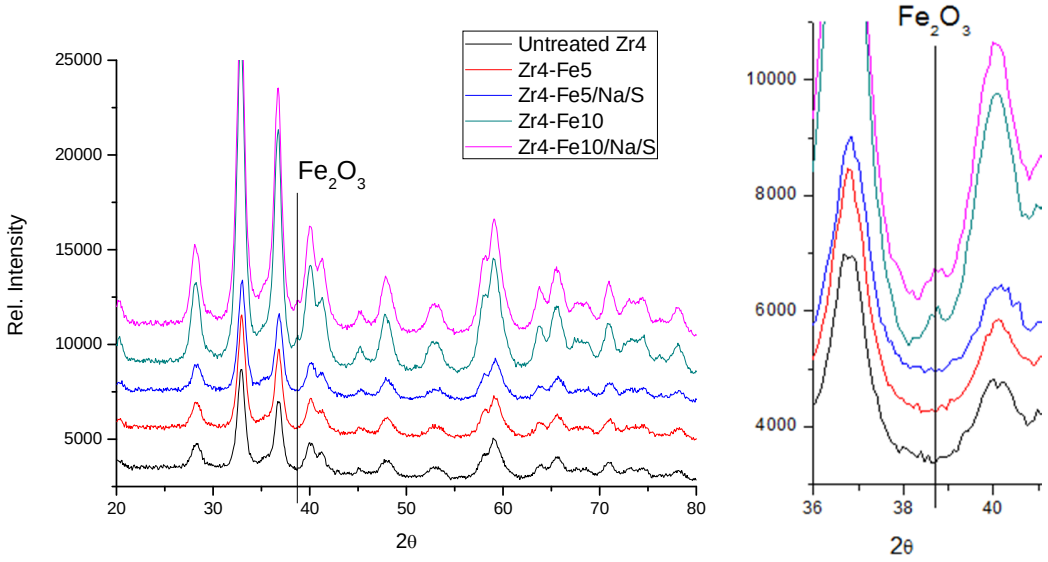

Figure 15: XRD diffractograms of Zr4 supported samples with inset zoomed on highest intensity hematite peak

To test the effect of higher loadings, both a doubly promoted and unpromoted 10wt% iron loaded catalyst was produced on Zr4, however their synthesis met with issues. The pore volume of the Zr4 support was insufficient to contain the amount of iron precursor required for a 10wt% loading, resulting in loss of precursor and external nucleation. The actual obtained iron loading of these samples is therefore likely lower than the projected 10wt%. After calcination and sieving these samples were investigated by XRD and TEM. The XRD diffractograms, shown above in Figure 15, indicate that in contrast with the 5wt% Fe loading samples, the prepared catalysts with a higher iron loading hematite particles are present. This supports the possibility of external nucleation.

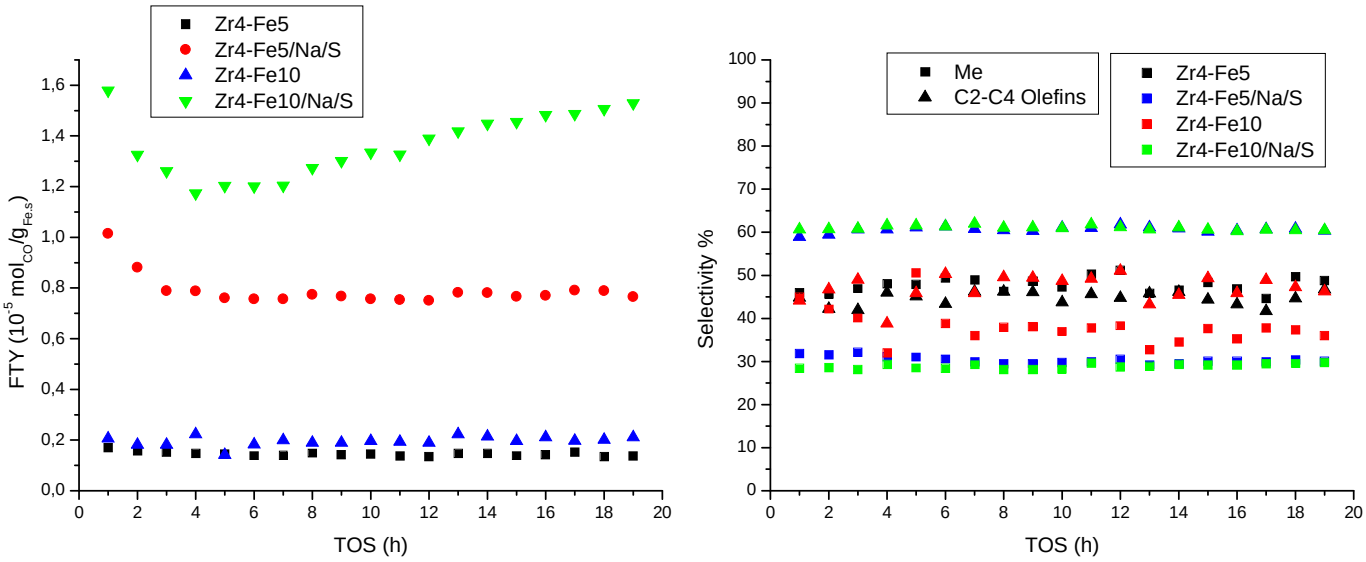

Figure 16: Comparison of activity and selectivity over time on stream of Zr4 supported catalysts with 5wt% or 10wt% iron loading

In catalytic activity testing, the increase in iron loading also shows variable success. As shown in Figure 16, the unpromoted catalyst with increased loading is roughly as effective as a sample with half its iron content. In the promoted catalyst, a peculiar activity trend is found. After the initial high activity and subsequent stabilization, comparable to a 5wt% loading sample, the activity starts to steadily increase. It may be possible this is due to blocked pores becoming available again.

The singly promoted catalysts performed as expected[14], with the sodium-only promoted sample increasing chain growth probability but not activity, and the sulphur-only promoted catalyst greatly increasing activity as well as decreasing methane selectivity. The Zr4-supported catalysts performance for the 1 bar Fischer-Tropsch reaction are summarized in Table 5.

Table 5: 1 bar Fischer-Tropsch activity and selectivity of all Zr4-supported catalysts after 15h on stream

	FTY (10-5molCO/gFe.s)	Selectivity %			
Sample		Me	C2-C4 Olefin	C2-C4 Paraffin	C5+
Zr4-Fe5	0,139	48,279	44,390	1,082	6,249
Zr4-Fe5/Na/S	0,766	30,099	60,145	1,819	7,937
Zr4-Fe5/Na	0,137	35,091	52,378	2,651	9,881
Zr4-Fe5/S	0,833	31,858	57,009	2,511	8,623
Zr4-Fe10	0,098	37,625	49,315	1,298	11,762
Zr4-Fe10/Na/S	0,728	29,123	60,612	2,146	8,118

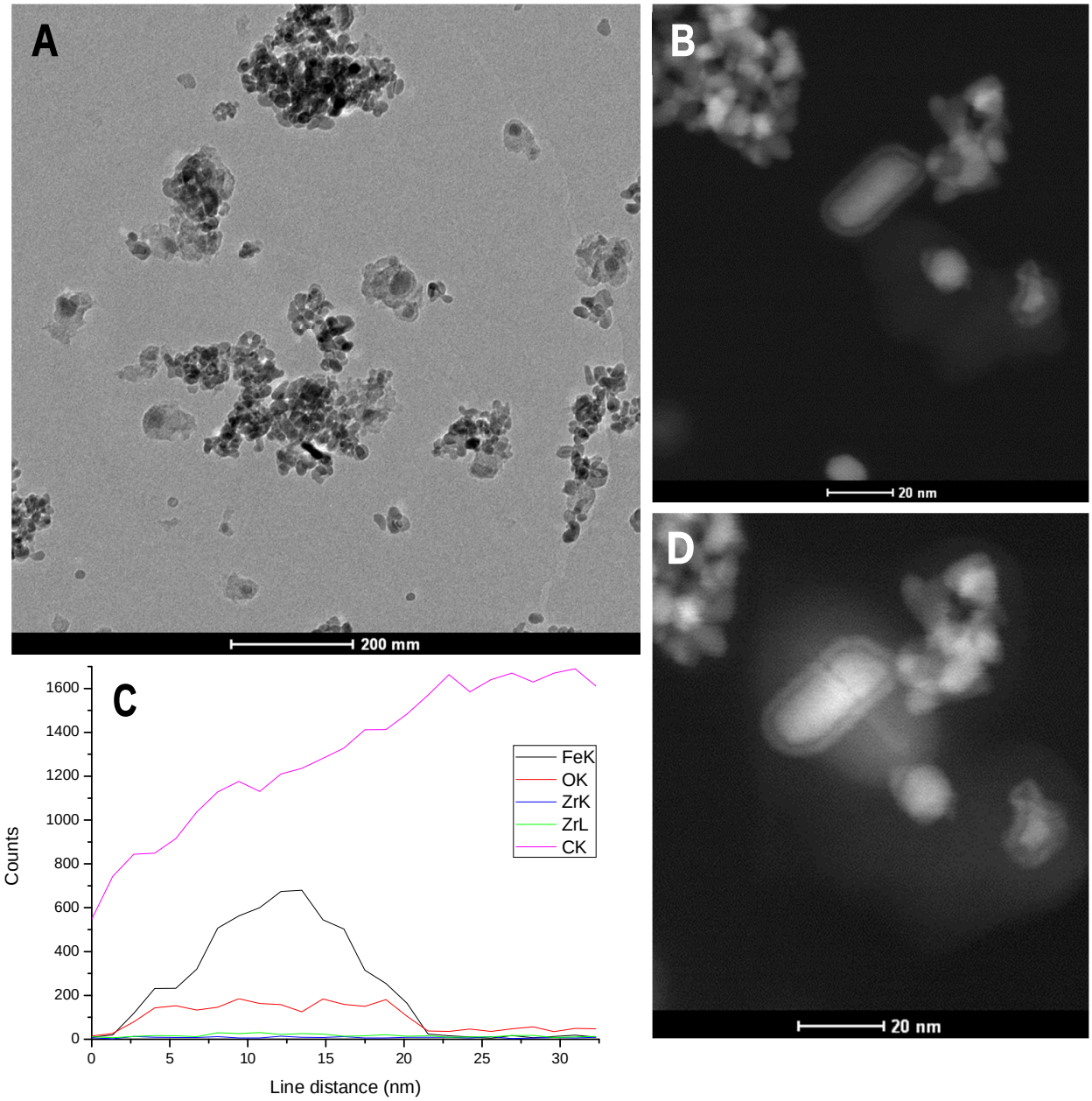

Figure 17: TEM overview image of a spent Zr4-Fe5/Na/S catalyst (A) showing zirconia crystallite clusters and separate iron particles with surrounding carbon growth, HAADF-STEM images of large iron particle before (B) and after (D) EDX line scan depicted in graph (C)

Spent catalysts from FTO runs were collected and investigated using TEM-EDX to determine the possible degradation of catalyst structure after reaction. Shown above in Figure 17 is a representative TEM image obtained of a spent catalyst. Amorphous material, presumed to be carbon growth, was observed near to particle clusters, but also surrounding separate particles, which deviated in size from the support crystallites. Many of these separate particles, expected to be iron particles, also appeared to have a shell. HAADF-STEM-EDX line scans were performed to investigate the makeup of these particles. Due to the fact that the TEM sample is prepared on a carbon sticker, it was impossible to determine whether iron carbide was present as beam damage polluted the carbon signal, which can be seen in the EDX line scan

also shown above. Based on the obtained data, it is suggested that the particles were in fact iron metal particles with an iron oxide shell, as the oxygen signal only increases in concert with the iron signal at the shell, remaining stable through the center of the particle.

As it was unclear whether the carbon growth found in spent catalysts occurred during reaction or during the cooldown from reaction conditions to room temperature, possibly due to the breakdown of iron carbide, FT reactions were performed with a cooldown step to determine whether this impacted catalyst performance afterwards. Starting off as a regular Fischer-Tropsch run, after 5 hours on stream the sample was cooled down to room temperature, after which it is reheated and the reaction was continued.

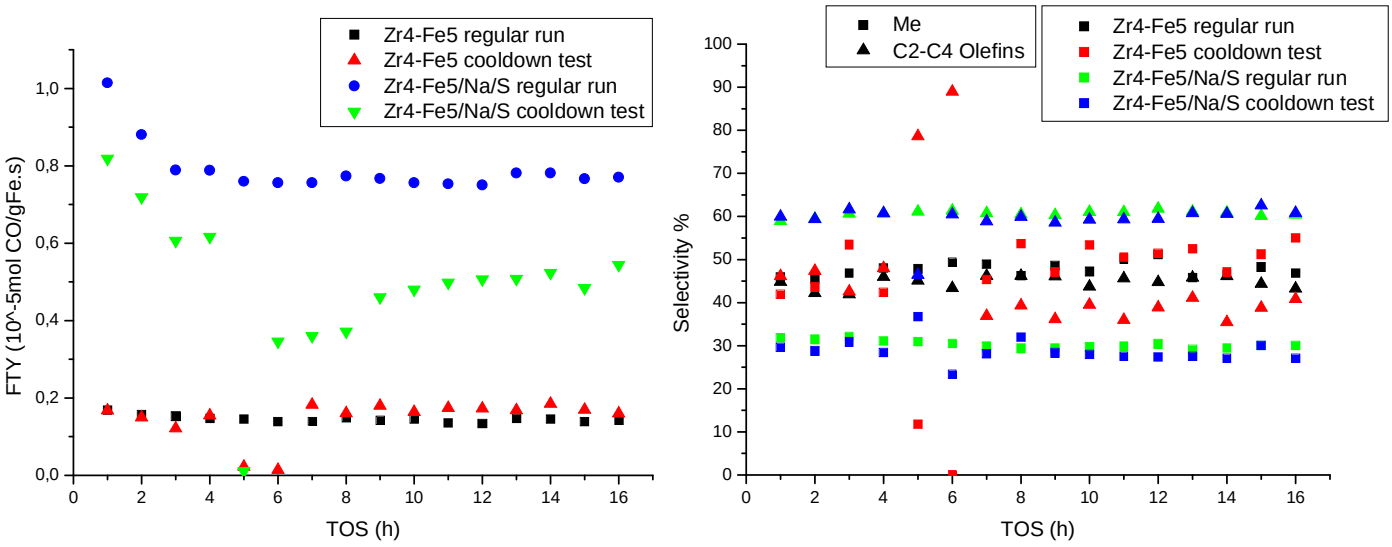

Figure 18: Comparison of activity and selectivity over time on stream between regular and a cooldown runs

In Figure 18, the tests show that for an unpromoted sample, there is very little difference between a regular run and a run with a mid-measurement cooldown; methane selectivity is somewhat higher and olefin selectivity is lower, whilst the activity is approximately the same. However, for the promoted sample, whilst the selectivity shows no change, the activity is roughly halved directly after the cooldown, after which it slowly increases back to approach pre-cooldown levels. This indicates a deactivation of the catalyst caused by the cooldown, with a slow re-activation when brought back to reaction conditions. The increasing activity trend of the promoted sample shows similarities with the 10wt% iron loaded samples. It is possible that the cooldown resulted in the aggregation of iron into larger particles which then become fully active more slowly. As both in the 10wt% samples and in the cooldown tests only the promoted samples show this upward trend in activity whilst selectivity remains unchanged, it appears that in samples where larger iron particles are presumed to be present, promoters somehow affect the number of available active sites over time, or increase their turnover.

TPR measurements were performed on Zr4 supported catalysts, both unpromoted and doubly promoted, to investigate the effect of promoters on the rate and extent of reduction. As can be seen from the results detailed in Figure 19 below, on the zirconia supported samples there are two clear reduction steps which are tentatively assigned to Fe^{3+} to Fe^{2+} and subsequently to Fe^{0}. The addition of promoters appears to not have a great effect on the reduction profile as the onset of the first reduction step is slightly delayed whilst the second reduction step does occur more rapidly, indicating that the reduction to metallic iron on a zirconia support is somewhat more facile in the presence of promoters. For both samples, no further reduction took place approximately 20 minutes after the end temperature of 500°C was reached.

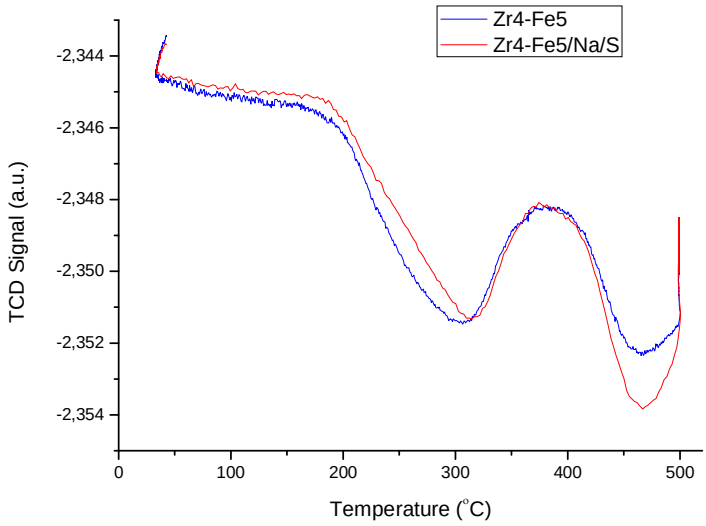

Figure 19: TPR reduction profiles of Zr4 supported unpromoted and doubly promoted catalysts

Both Boot *et al.*[25] and Berg *et al.*[23] report more complex reduction patterns of zirconia supported iron. Boot suggests bimodal particle distribution is the cause of the complex pattern, whilst Berg points out that the reduction does not proceed through a magnetite phase resulting in two main reduction regions, with the location and shape of the regions influenced by heating rate and hydrogen partial pressure.

Zr4 DRIFTS investigations:

DRIFTS measurements ran on the Zr4 supported catalysts are shown below in Figure 20. The IR spectra show the two previously mentioned regions of interest: in 2100-1800 cm^{-1} the signal from CO adsorbed on a surface can be found. There appears to be very little shift in frequency of the various adsorbed CO peaks, indicating that the promoters do not influence the binding strength of CO. What can be observed though is a change in relative intensity between the various bound states of CO, indicating a different distribution of bound states. This could mean that the promoters enhance or block certain binding sites. Besides this, again carbonate species are present in the 1700-1200 cm^{-1} region. However, as these peaks do not relate to the catalytic performance or the promoter effect of the sample, they will not be discussed further.

Deconvolution was attempted on the unpromoted and doubly promoted. Table 6 shows the deconvoluted peaks and their height/area. As can be seen, in both samples roughly the same peaks are present, however with differing relative intensity. To be able to account for the number of separate peaks, there appear to be a multitude of binding sites with different binding energies present. The deconvoluted spectra images can be found in Figure S3. 2044, 2006, 1971, 1913 and 1889 cm^{-1} are the main contributing peaks, whilst the remainder is hard to nail down definitively due to extensive overlap.

Peaks between 2050 and 2000 cm^{-1} are generally attributed to CO linearly bound to Fe^0 sites and peaks between 2150 and 2050 cm^{-1} to CO bound to ionic species. The peaks at 2044 and 2006 cm^{-1} are assigned to linearly bound Fe^0 – CO species, whilst 1971, 1913 and 1889 cm^{-1} are assigned to bridged-bonded CO species.[16]

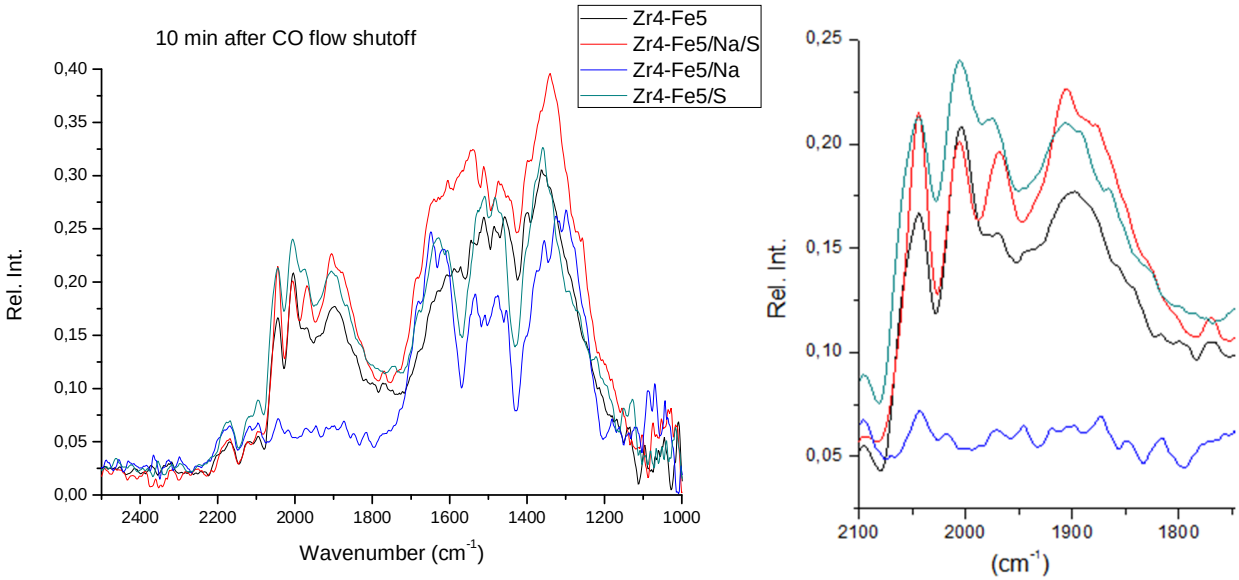

Figure 20: DRIFTS signal comparison with inset showing adsorbed CO region

Due to the well-dispersed nature of the iron present, it is very likely that small clusters of iron and iron carbonyls are formed. Guglielminotti conducted ^{13}CO-^{12}CO adsorption experiments on zirconia supported iron samples, and found mixed isotope groups were present, indicating the presence of iron polycarbonyl species.[30]

Exact peak assignment is difficult due to inconsistency in literature and only partial agreement between literature and experiment. Bian *et al.* report for a H_2 reduced precipitated iron catalyst only two significant peaks at 2033 and 2013 cm^{-1} assigned to linearly adsorbed Fe^0-CO.[31,32] Jiang *et al.* observe two linear (2043 and 2025 cm^{-1}) and one bridged (1896 cm^{-1}) adsorbed CO species, and assign them to $Fe_3(CO)_{12}$ iron carbonyl clusters. Guglielminotti, studying iron supported on zirconia, attributes peaks in the range of 2100-1990 cm^{-1} to $Fe_x(CO)_y$ clusters and adsorption at 1990-1970 cm^{-1} to Fe^0-CO species on extended faces of larger crystals with minor contributions in the 2030-2020 cm^{-1} range. The bands at 1868-1853 cm^{-1} are also assigned to the bridged CO species of $Fe_3(CO)_{12}$.[30]

Table 6: Deconvoluted peak information of DRIFTS spectra

Zr4Fe5				Zr4Fe5/Na/S		
Peak Center	Peak Area	Peak Height		Peak Center	Peak Area	Peak Height
				1802	0,12	0,01
				1815	0,36	0,02
				1829	0,45	0,03
1848	0,83	0,03		1849	1,79	0,06
1858	0,07	0,01				
1871	0,92	0,04		1873	2,58	0,08
1889	1,75	0,06				
1913	2,58	0,08		1907	6,47	0,14
1940	1,47	0,05		1938	0,59	0,03
1971	3,05	0,08		1969	5,01	0,12
2006	4,56	0,14		2008	3,57	0,12
2044	2,74	0,11		2044	3,84	0,15
2061	0,86	0,05		2065	0,3	0,02

Thus it is argued that due to the difficult reduction caused by the oxide-oxide interaction between support and the iron, relatively small amounts of iron^0 are formed, reducing the chance of large particle formation. The lack of significant peaks in the multiply-bonded region (1800-1650 cm^{-1}) also indicates that the iron particles are likely to be small.[19] However due to the extensive overlap, it is likely that there is a mixture of a minor amount of larger particles with extended crystal faces and fine clusters forming iron carbonyls present.

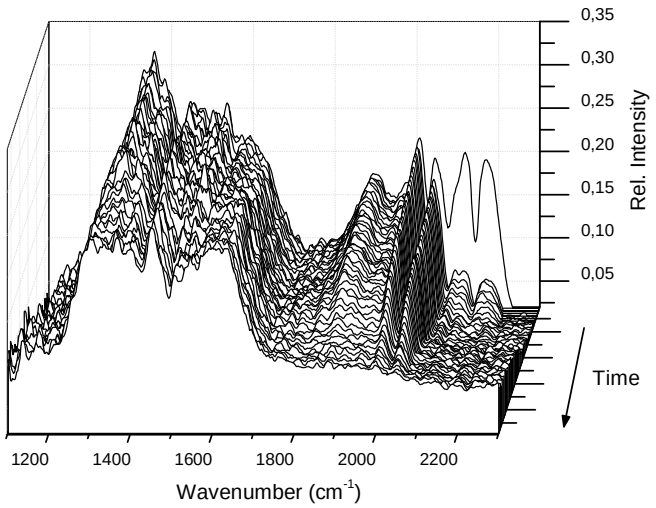

Figure 21: Development over time of IR spectrum of Zr4-Fe5 catalyst

The development in time of the peaks, after switching to a He flow, is shown above in Figure 21. Gaseous CO is the first to dissipate, the peaks disappearing after roughly 10 minutes. The bound CO disappears slowly over the course of 16 hours, with no discernable difference between peaks, whilst the carbonates remain relatively stable over time. This means that multiply bonded CO appears to dissociate at the same rate as linearly bonded CO.

It should be noted that these measurements measure the interaction between metallic iron and CO, as the catalyst is only reduced. However, the active phase of the catalyst is iron carbide. Therefore, steps were undertaken to approach the active phase and study its' interaction with CO. A carburization step was performed after reduction in situ; putting the sample under reaction conditions (6 mL/min H_2/CO flow, 1:1 v/v) at 350°C for a varying amount of time. Additionally in a separate protocol the catalyst was reduced with CO instead of H_2, instigating the formation of iron carbide during reduction instead of during reaction conditions. Shown below is a comparison of the obtained DRIFTS spectra of these carburization investigations.

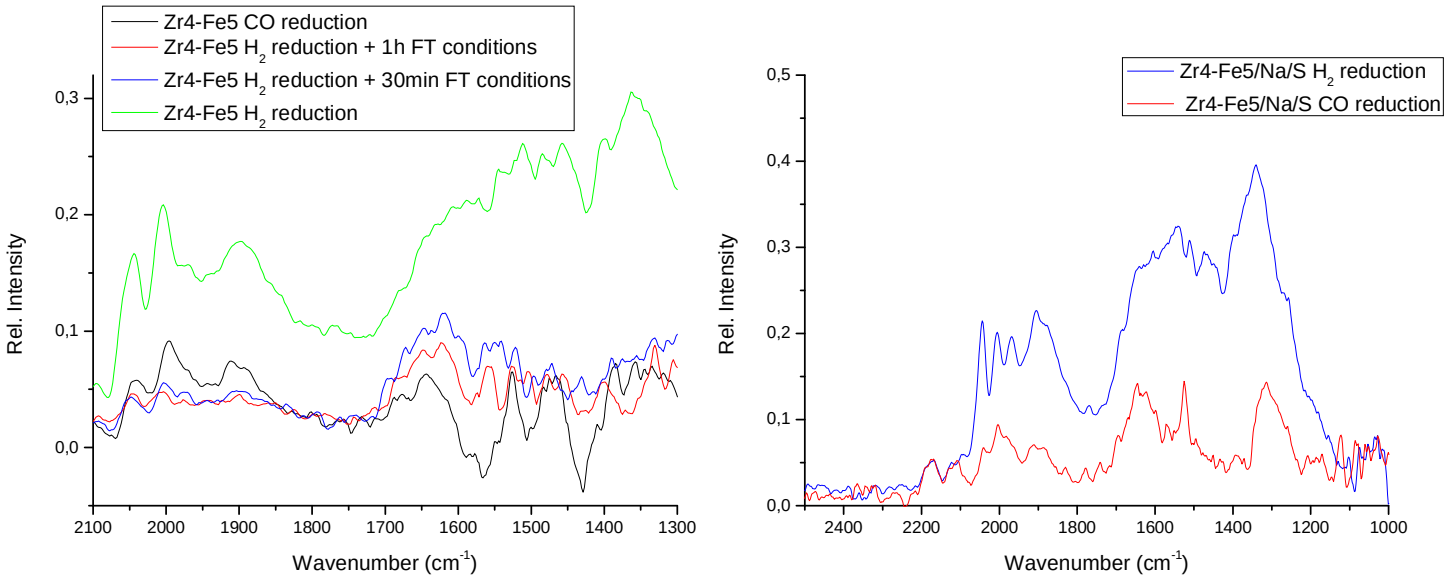

Figure 22: DRIFTS spectra obtained of Zr4-Fe5 and Zr4-Fe5/Na/S catalysts with different pretreatment. Measurements were taken 10 minutes after shutting off the CO flow

The signal was significantly lower, as shown in Figure 22. This could be due to carbon deposition during reduction lowering the reflectivity of the sample, the darkening of the sample as the iron oxide transforms to metallic iron or iron carbide during and after reduction or due to increased dissociation of CO on the formed iron carbide species.[32] A comparison of obtained background spectra is shown in the supplementary information (S4) and shows that the desorption step was successful in removing leftover CO from the reduction, as there is no adsorption difference in the bound CO region; thus the background did not influence the measured intensity. The background of the CO reduced sample does show a higher intensity in the carbonate region. As the presence of CO is expected to cause the formation of carbonates and as these were shown to be more stable, this is not unexpected and is the cause of the much lower and even negative intensity in the carbonate region in the measurement.

As can be seen, the difference in pretreatment does not appear to influence the adsorbed CO peaks, either in wavenumber or relative intensity, apart from possible larger shoulders in the 2050-1950 cm^{-1} region. This could mean that the pretreatment does not significantly affect the available binding sites present for CO. However, the CO reduction is expected to result in iron carbide formation. Bian *et al.*[31] identify peaks at 1999 and 2021 cm^{-1} caused by CO adsorbed on iron carbide. It is entirely possible that these peaks are present, however due to the low signal and significant overlap this is impossible to ascertain. Thus although plausible, it is not possible to show CO adsorbed on iron carbide.

Attempts to increase the signal in IR measurements were undertaken by increasing the iron loading or to dilute the measured sample with highly reflective alumina, but were not successful. Transmission IR was also attempted as an alternative, however due to severe difficulty in obtaining a suitable pellet for measurement this was not continued. Catalysts with higher iron loadings (10wt%) were initially also synthesized on the Zr1 support during the pilot but as the support was deemed unsuitable the effect of their increased loading in IR measurements was never tested. The Zr4-Fe10 and Zr4-Fe10/Na/S samples were also measured in DRIFTS, however they failed to return a usable signal.

Additionally, Mössbauer measurements were performed on an unpromoted and a doubly promoted Zr4 catalyst mimicking the experimental conditions of the DRIFTS measurements, to determine the phases present and assist in determining the binding sites. Shown in Table 7 are the results and the spectra can be found in supplementary info, Figure S5. After 2 hours of reduction under H_2, both samples contain a mixture of Fe^0, Fe^{2+} and Fe^{3+}, although the promoted sample has a higher extent of reduction, supporting the TPR results. However, when the sample is cooled down to room temperature and subsequently subjected to 30 minutes of CO flow, it can be noted that all of the presumably unstable Fe^{2+} has degenerated back to the Fe^{3+} state. Also of note is that no iron carbide is formed after the exposure to CO at room temperature, which confirms the requirement of a carburization step to enable the option of studying the relevant active phases in the DRIFTS measurements.

Sample	*IS* ($mm \cdot s^{-1}$)	*QS* ($mm \cdot s^{-1}$)	*Hyperfine field (T)*	*Γ* ($mm \cdot s^{-1}$)	*Phase*	*Spectral contribution (%)*
5FeZrO2 Fresh	0.34	0.88	-	0.50	Fe^{3+}	100
5FeZrO2	0.01	-	33.3	0.28	Fe^0	39
H_2/Ar, 350 °C	0.39	0.88	-	0.60	Fe^{3+}	28
	1.02	1.90	-	0.64	Fe^{2+}	33
5FeZrO2	0.01	-	33.3	0.29	Fe^0	37
CO, RT	0.35	0.99	-	0.54	Fe^{3+}	63
30 min.						
5PFeZrO2 Fresh	0.35	0.87	-	0.53	Fe^{3+}	100
5PFeZrO2	0.01	-	33.3	0.27	Fe^0	52
H_2/Ar, 350 °C	0.45	0.75	-	0.76	Fe^{3+}	26
	0.95	1.98	-	0.59	Fe^{2+}	22
5PFeZrO2	0.01	-	33.3	0.29	Fe^0	49
CO, RT	0.34	0.97	-	0.57	Fe^{3+}	48
30 min.	1.05	2.07	-	0.30	Fe^{2+}	3

Table 7: Experimental uncertainties: Isomer shift: I.S. ± 0.01 mm s-1; Quadrupole splitting: Q.S. ± 0.01 mm s-1; Line width: Γ ± 0.01 mm s-1; Hyperfine field: ± 0.1 T; Spectral contribution: ± 3%.

Conclusions:

The investigation into the promoter effect of Na and S on a supported iron catalyst using CO-probe IR spectroscopy showed that it is plausible that the promoters influence the crystal structure of iron metal particles or block different adsorption sites, thereby possibly reducing methane formation below the level predicted by the ASF distribution and limiting chain propagation. However, the effect of the promoters on the catalytically active carbide phase has not been determined as efforts to measure carburized samples with DRIFTS were unsuccessful. Mössbauer and TPR results have shown that the promoters increase the rate of reduction of iron.

Zirconia as a support for an iron-based FTO catalyst is a viable high-surface area alternative to more prevalent supports such as α-alumina. The promoter effect is present both in low pressure and medium pressure, high throughput catalytic testing. Iron oxide enters a solid solution with the surface of the support, ensuring a high dispersion and a strong anchoring of iron, although catalyst stability is not optimal as particle growth and carbon deposition reduce effectiveness.

Future outlook:

In order to further support the viability of zirconia as a support for the FTO reaction, longer duration reaction testing should be performed to further investigate catalyst stability. An effort could be made to further investigate the promoter effect on the active phase of the catalyst, improving carburization steps or investigating additional techniques; Further Mössbauer and IR measurements of singly promoted samples could illuminate the individual effects of the promoters.

Acknowledgements:

I would like to thank Jingxiu Xie (JX) for accepting me to work on her project and her supervision and guidance during the project. Prasad Gonogunta for his hands-on assistance with the DRIFTS measurements in Delft, Iulian Dogolan for his help setting up the DRIFTS measurements, valuable input and the Mössbauer measurements, Hans Meeldijk for his help in TEM imaging sessions and Prof. Krijn de Jong as project supervisor and for the helpful discussions and invaluable suggestions.

Bibliography:

1. Galvis, H. M. T. & Jong, K. P. De. Catalysts for Production of Lower Olefins from Synthesis Gas : A Review. *ACS Catal.* **3,** 2130–2149 (2013).

2. Van Santen, R. a, Markvoort, a J., Filot, I. a W., Ghouri, M. M. & Hensen, E. J. M. Mechanism and microkinetics of the Fischer-Tropsch reaction. *Phys. Chem. Chem. Phys.* **15,** 17038–63 (2013).

3. De Smit, E. & Weckhuysen, B. M. The renaissance of iron-based Fischer-Tropsch synthesis: on the multifaceted catalyst deactivation behaviour. *Chem. Soc. Rev.* **37,** 2758–2781 (2008).

4. Ding, M. *et al.* Transformation of carbonaceous species and its influence on catalytic performance for iron-based Fischer–Tropsch synthesis catalyst. *J. Mol. Catal. A Chem.* **351,** 165–173 (2011).

5. Lee, D.-H. *et al.* Correlation of the amount of carbonaceous species with catalytic performance on iron-based Fischer–Tropsch catalysts. *Fuel Process. Technol.* **109,** 141–149 (2012).

6. Cano, L. a. *et al.* Fischer-Tropsch synthesis. Influence of the crystal size of iron active species on the activity and selectivity. *Appl. Catal. A Gen.* **379,** 105–110 (2010).

7. Zhang, Q., Kang, J. & Wang, Y. Development of Novel Catalysts for Fischer-Tropsch Synthesis: Tuning the Product Selectivity. *ChemCatChem* **2,** 1030–1058 (2010).

8. Qing, M. *et al.* Modification of Fe–SiO2 interaction with zirconia for iron-based Fischer–Tropsch catalysts. *J. Catal.* **279,** 111–122 (2011).

9. Li, J. *et al.* Effects of alkaline-earth metals on the structure, adsorption and catalytic behavior of iron-based Fischer–Tropsch synthesis catalysts. *Appl. Catal. A Gen.* **464-465,** 10–19 (2013).

10. Lohitharn, N., Goodwin, J. G. & Lotero, E. Fe-based Fischer-Tropsch synthesis catalysts containing carbide-forming transition metal promoters. *J. Catal.* **255,** 104–113 (2008).

11. Coville, N. J. & Bromfield, T. C. The effect of sulfide ions on a precipitated iron Fischer–Tropsch catalyst. *Appl. Catal. A Gen.* **186,** 297–307 (1999).

12. McCue, A. J. & Anderson, J. a. Sulfur as a catalyst promoter or selectivity modifier in heterogeneous catalysis. *Catal. Sci. Technol.* **4,** 272–294 (2014).

13. Torres Galvis, H. M. *et al.* Supported iron nanoparticles as catalysts for sustainable production of lower olefins. *Science (80-.).* **335,** 835–838 (2012).

14. Torres Galvis, H. M. *et al.* Effects of sodium and sulfur on catalytic performance of supported iron catalysts for the Fischer–Tropsch synthesis of lower olefins. *J. Catal.* **303,** 22–30 (2013).

15. Ryczkowski, J. IR spectroscopy in catalysis. *Catal. Today* **68,** 263–381 (2001).

16. Hollins, P. The influence of surface defects on the infrared spectra of adsorbed species. *Surf. Sci. Rep.* 51–94 (1992).

17. Curtis, V., Nicolaides, C. P., Hildebrandt, D., Coville, N. J. & Glasser, D. The effect of sulfur on supported cobalt Fischer–Tropsch catalysts. *Catal. Today* **49,** 33–40 (1999).

18. Morales, F., de Smit, E., de Groot, F. M. F., Visser, T. & Weckhuysen, B. M. Effects of manganese oxide promoter on the CO and H2 adsorption properties of titania-supported cobalt Fischer–Tropsch catalysts. *J. Catal.* **246,** 91–99 (2007).

19. Jiang, M., Koizumi, N. & Yamada, M. Adsorption Properties of Iron and Iron - Manganese Catalysts Investigated by in-situ Diffuse Reflectance FTIR Spectroscopy. 7636–7643 (2000).

20. Kazansky, V. B., Zaitsev, a. V., Borovkov, V. Y. & Lapidus, a. L. Infrared diffuse reflectance study of alkali promoted iron/alumina and cobalt/alumina Fischer-Tropsch catalysts prepared by decomposition of carbonyls. *Appl. Catal.* **40,** 17–25 (1988).

21. Dillen, A. Van, Terörde, R., Lensveld, D., Geus, J. & Jong, K. P. De. Synthesis of supported catalysts by impregnation and drying using aqueous chelated metal complexes. *J. Catal.* **216,** 257–264 (2003).

22. Berg, F. R. Van Den, Crajé, M. W. J., Kooyman, P. J., Kraan, A. M. Van Der & Geus, J. W. Synthesis of highly dispersed zirconia-supported iron-based catalysts for Fischer – Tropsch synthesis. *Appl. Catal. A Gen.* **235,** 217–224 (2002).

23. Berg, F. R. Van Den, Crajé, M. W. J., Kraan, A. M. Van Der & Geus, J. W. Reduction behaviour of Fe / ZrO 2 and Fe / K / ZrO 2 Fischer – Tropsch catalysts. *Appl. Catal. A Gen.* **242,** 403–416 (2003).

24. Chen, K., Fan, Y., Hu, Z. & Yan, Q. Carbon monoxide hydrogenation on Fe203 / ZrO2 catalysts. *Catal. Letters* **36,** 139–144 (1996).

25. Boot, L. A., Dillen, A. J. Van, Geus, J. W. & Buren, F. R. Van. Iron-Based Dehydrogenation Catalysts Supported on Zirconia. *J. Catal.* **163,** 186–194 (1996).

26. Popov, V. V. Mössbauer spectroscopy of interfaces in metals. *Phys. Met. Metallogr.* **113,** 1257–1289 (2012).

27. Chorkendorff, I. & Niemantsverdriet, J. W. *Concepts of Modern Catalysis and Kinetics*. *Adsorpt. J. Int. Adsorpt. Soc.* (WILEY-VCH Verlag GmbH & Co. KGaA,Weinheim, 2003).

28. Collins, J. F. & Ferguson, I. F. Lattice parameter variations in mixed oxides with the monoclinic zirconia structure: The systems ZrO2-Fe2O3, ZrO 2-SnO2, and ZrO2-Cr2O3. *J. Chem. Soc.* 4–5 (1968).

29. Guglielminotti, E. Infrared Study of Syngas Adsorption on Zirconia. **71,** 1455–1460 (2000).

30. Guglielminotti, E. Spectroscopic Characterization of the Fe / Zr02 System . 1 . CO Adsorption. *J. Phys. Chem.* **98,** 4884–4891 (1994).

31. Bian, G., Oonuki, A., Kobayashi, Y., Koizumi, N. & Yamada, M. Syngas adsorption on precipitated iron catalysts reduced by H2, syngas or CO and on those used for high-pressure FT synthesis by in situ diffuse reflectance FTIR spectroscopy. *Appl. Catal. A Gen.* **219,** 13–24 (2001).

32. Bian, G., Oonuki, A., Koizumi, N., Nomoto, H. & Yamada, M. Studies with a precipitated iron Fischer-Tropsch catalyst reduced by H2 or CO. *J. Mol. Catal. A Chem.* **186,** 203–213 (2002).

33. Adapted from: http://photonicssociety.org/newsletters/apr98/nearinfrared.htm (Retrieved 01-07-2014).

Supplementary data:

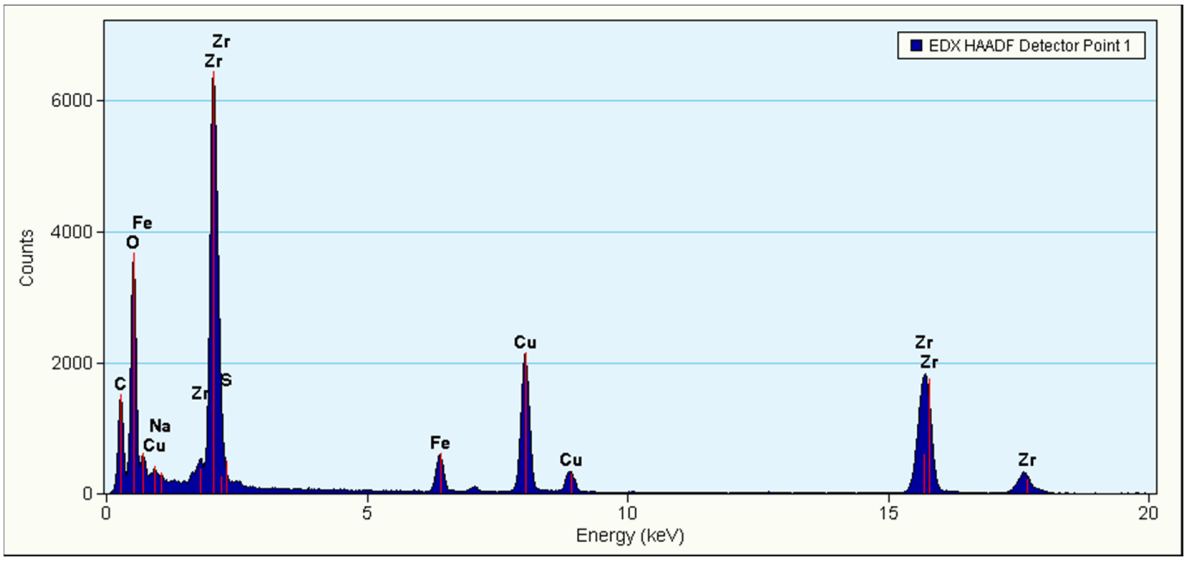

Figure S1: bulk EDX spectrum of Zr1-Fe5/Na/S catalyst, confirming the presence of iron

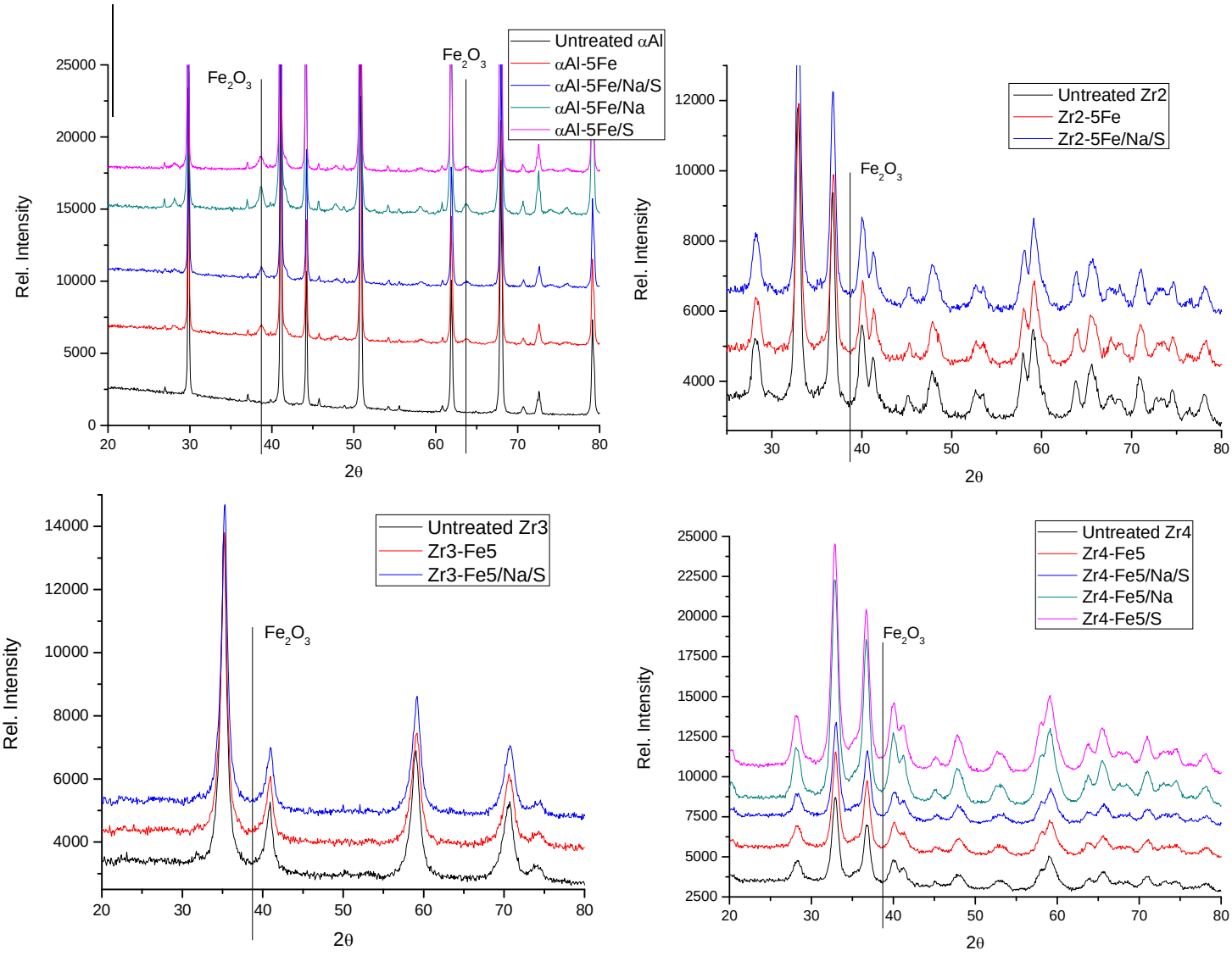

Figure S2: XRD diffractograms of prepared catalysts supported on the various employed supports, with only α-alumina supported samples displaying the presence of hematite

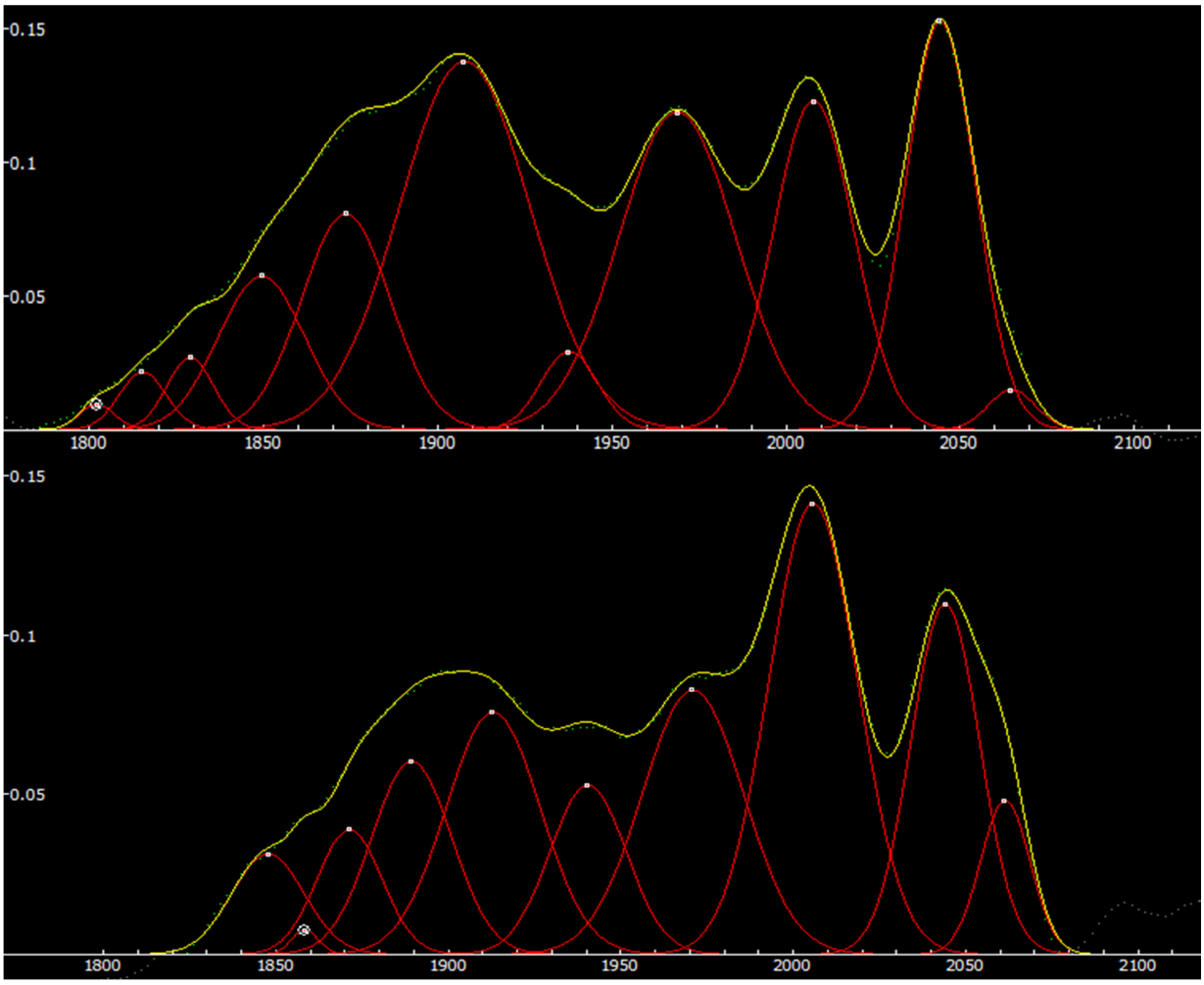

Figure S3: Deconvoluted DRIFTS spectra of Adsorbed CO region. Zr4-Fe5/Na/S is shown above and Zr4-Fe5 below

I

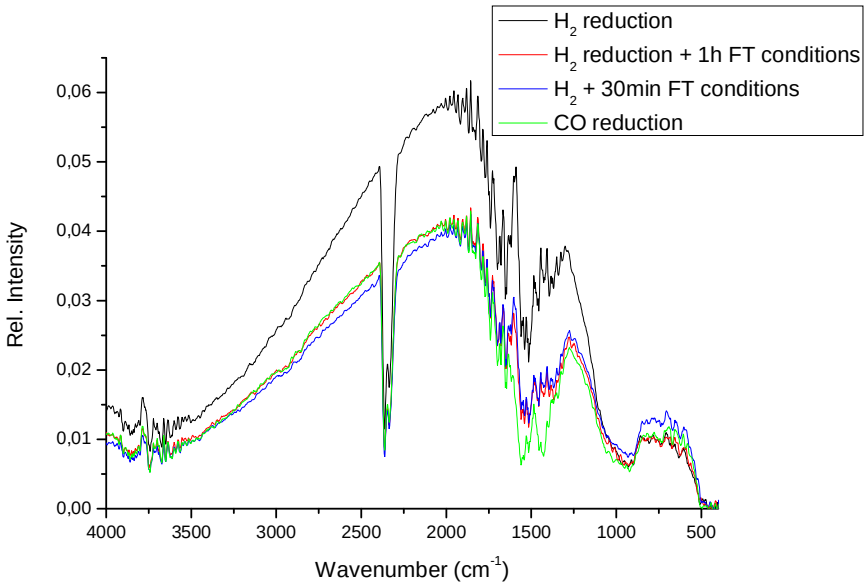

Figure S4: Background spectra of the various Zr4-Fe5 DRIFTS measurements showing no CO presence before the start of the actual measurement

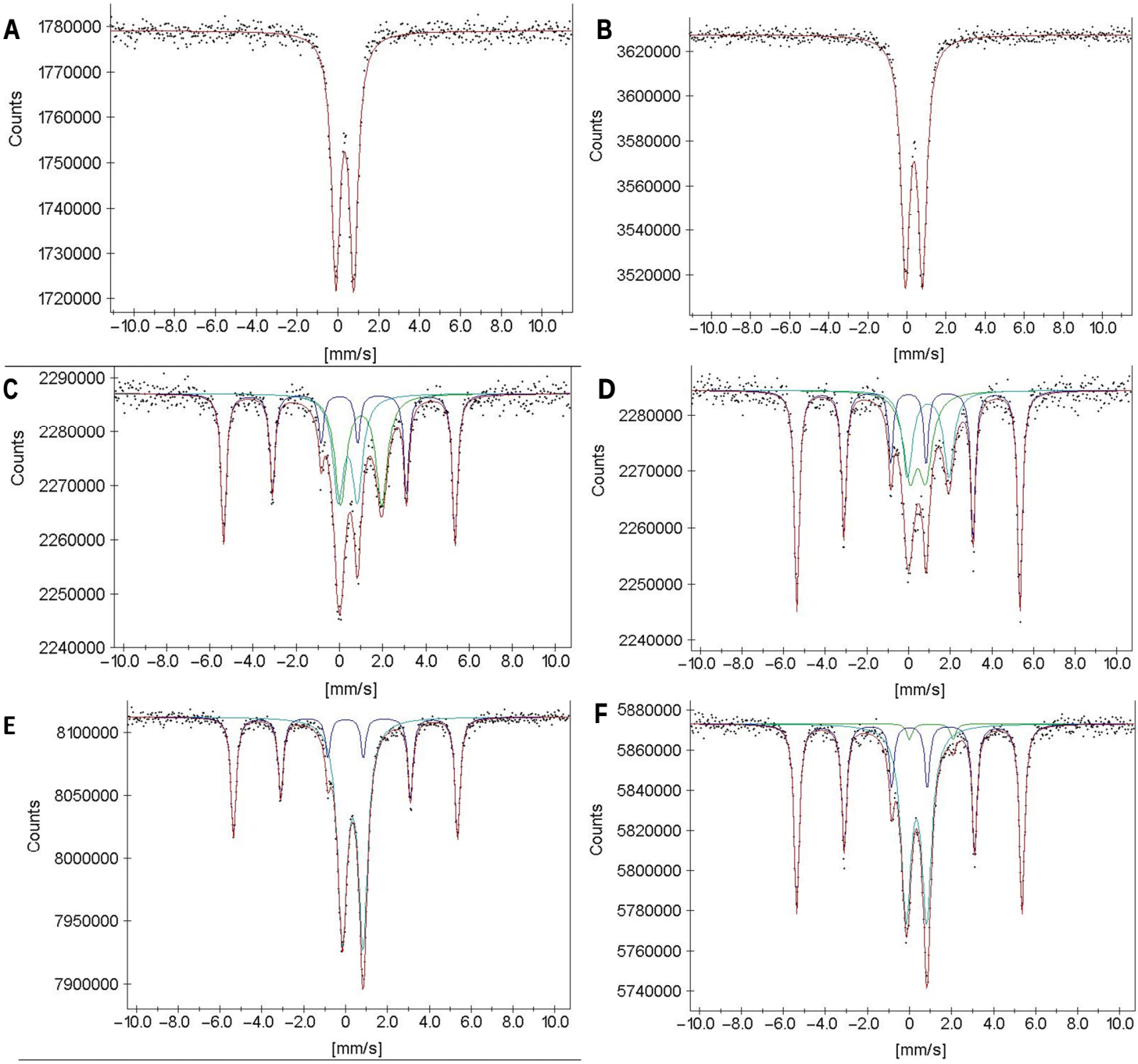

Figure S5: Obtained Mössbauer spectra. A, C, E are from 5FeZrO2 catalyst; B, D, F are from 5PFeZrO2 catalyst. A/B are obtained at 300K from a fresh sample, C/D at 300K after 2 hours of H2 reduction; E/F at 300K after 30 min of CO exposure at RT.